PONTIFICIA UNIVERSIDAD CATÓLICA DE CHILE

Facultad de Ciencias Biológicas
Programa de Doctorado en Ciencias Biológicas
Mención Genética Molecular y Microbiología

"Identificación y Caracterización de los mecanismos moleculares involucrados en el control de la distribución y almacenamiento de hierro durante el desarrollo de semillas de *Chenopodium quinoa*"

Tesis entregada a la Pontificia Universidad Católica de Chile en cumplimiento parcial de los requisitos para optar al Grado de Doctor en Ciencias con mención en Genética Molecular y Microbiología

Por:

MIGUEL ÁNGEL IBEAS HENRÍQUEZ

Director de tesis: Dr. Hannetz Roschzttardtz

Santiago, Chile.
Septiembre, 2020

RESUMEN

El hierro es un micronutriente esencial para casi todos los organismos vivos. Los embriones acumulan hierro durante la etapa de maduración de la semilla de la embriogénesis. El déficit de hierro es un gran problema agronómico ya que afecta la rdesarrollo de las plantas y limita de fertilidad y rendimiento de los cultivos. Utilizando embriones de *Arabidopsis thaliana* ha sido posible determinar que el hierro se acumula específicamente en las vacuolas de las células de la endodermis. Utilizando la tinción Perls/DAB, fuimos capaces de identificar que este patrón de distribución es diferente en otros miembros de las Brassicales. Nosotros extendimos este estudio a embriones de especies pertenecientes a distintos órdenes de las Eudicotyledoneae. Nuestros resultados sugieren que el patrón de distribución de hierro observado en embriones de Arabidopsis no es conservado en otras Eudicotyledoneae. Notablemente, en embriones de *Chenopodium quinoa* el hierro se acumula en distintas capas celulares incluyendo las células del cortex y la endodermis. Interesantemente, identificados una gran cantidad de fitoferritinas en embriones de quinoa. *Chenopodium quinoa* es un pseudo-cereal de origen andino muy nutritivo que se caracteriza por crecer en diversos ecosistemas y ha alcanzado un alto nivel de atención debido a lo nutritivas de sus semillas. Por otro lado, nosotros observamos que durante el desarrollo de la semilla de *Chenopodium quinoa* el hierro se carga de una manera diferente a lo que observamos en el desarrollo de semillas de *Brassica napus.* Nuestros resultados abren nuevas preguntas respecto a cuáles son los mecanismos que controlan la carga, distribución y acumulación de hierro en semillas.

ABSTRACT

Iron is an essential micronutrient for all living organisms. Embryo accumulates iron during seed maturation stages of embryogenesis. The role of iron in seed yields is an important agronomical trait because iron deficiency affects plant reproduction and limit crops yields. Using *Arabidopsis thaliana* embryos, it has been described that iron accumulates in the vacuoles of the endodermis cell layer. Using Perls/DAB staining we were able to identify that this distribution pattern is conserved in different members from Brassicales. We extend this study to embryos belonging to species from different orders from Eudicotyledoneae. Our results suggest that iron pattern found in Arabidopsis is not extended to all Eudicotyledoneae. Noticeably, in *Chenopodium quinoa* embryos iron accumulates in several cell layers including cortex and endodermis cells. Interestingly, we detected high amount of phytoferritins in quinoa embryos. *Chenopodium quinoa* is a highly nutritious crop that is adapted to a wide range of ecosystems and it has reach international attention because of the nutritional value. We found that iron loading during *Chenopodium quinoa* seed development is different than what we observed before in embryos belonging to the Brassicaceae family. Ours results open new questions about the molecular mechanism controlling iron loading, distribution and accumulation in quinoa embryo seeds.

INTRODUCCIÓN

El hierro (Fe) es un micronutriente esencial para los organismos vivos. Las macromoléculas que contienen hierro poseen funciones en diversos procesos vitales para la célula como son la división y respiración celular, estabilidad y reparación del DNA, además de ser requerido como cofactor para un gran número de enzimas. Adicionalmente, las plantas necesitan Fe para la biosíntesis de clorofila y las reacciones de la fotosíntesis (Curie and Briat, 2003; Li and Lan, 2017). A pesar de ser uno de los micronutrientes más abundantes en los suelos, en condiciones aeróbicas y con pH neutro o básico el Fe forma de hidróxidos -una forma poco soluble- limitando drásticamente su biodisponibilidad (Grillet *et al.,* 2014).

El déficit de Fe es un problema de gran relevancia tanto desde el punto de vista agronómico como para la salud humana. La Organización Mundial de la Salud (OMS) ha estimado que alrededor del 30% de la población mundial padece de anemia por déficit de Fe (FDA por sus siglas en inglés por *Fe Deficiency-induced Anemia*), afectando principalmente a mujeres y niños menores de dos años (*USA National Institute of Health, Office of Dietary Supplements*, https://ods.od.nih.gov/factsheets/Iron-HealthProfessional/). Teniendo esto en consideración, el uso de biotecnología para modular el contenido de Fe en variedades de interés comercial se ha vuelto una alternativa para combatir la FDA, y para este fin, una mejor comprensión de los mecanismos de transporte y almacenamiento de Fe en los distintos tejidos vegetales es necesaria (Grillet *et al.,* 2014; Yu *et al.,* 2012).

Desde el punto de vista agronómico, en condiciones de déficit de hierro las plantas presentan retraso en el desarrollo acompañado de un fenotipo de clorosis internerval en el tejido vegetativo, reduciendo la tasa fotosintética y a su vez afectando el rendimiento y productividad del cultivo (Zhu *et al.,* 2016). Por otro lado, debido a las propiedades químicas del hierro y su capacidad de reaccionar con el oxígeno, el exceso de este micronutriente también es perjudicial para el desarrollo de organismos aeróbicos, causando una gran cantidad de desórdenes funcionales y daños celulares (Briat *et al.,* 2010). Las plantas han desarrollado sofisticados mecanismos para controlar la absorción, transporte y almacenamiento de hierro, y de esta manera obtener cantidades suficientes de este nutriente evitando alcanzar niveles tóxicos (Kobayashi and Nishizawa, 2012).

Dos distintas estrategias de captación de hierro han sido descritas. La estrategia I es utilizada por todas las plantas excepto por las gramíneas, y consta principalmente de aumentar la solubilidad del Fe mediante la excreción de protones a la rizósfera (Santi and Schmidt, 2009), la posterior reducción de Fe^{3+} a Fe^{2+} mediada por *Ferric Reduction Oxidase2* o *FRO2* (Robinson et al., 1999), y finalmente la incorporación de Fe^{2+} a la planta a través del transportador *Iron-Regulated Transporter1* o *IRT1* (Vert *et al.,* 2002). La estrategia II es utilizada principalmente por gramíneas y se basa en la captación de Fe complejado con fitosideróforos solubles (PS por sus siglas en inglés por *Phyto-Siderophores*) que poseen alta afinidad por Fe^{3+}. Los complejos PS-Fe^{3+}son rápidamente transportados hacia el interior de la epidermis de la raíz por un sistema de captación de alta afinidad mediado por el transportador *Yellow Stripe 1* o *YS1* (Schaaf *et al.,* 2004).

Una vez que es adquido por las raíces desde el suelo, este micronutriente es distribuido a los distintos tejidos y células de la planta. Poco se sabe respecto a los mecanismos que controlan la distribución de Fe a los distintos tejidos y organos. Recientemente fue posible identificar diversas proteínas transportadoras y ligandos de hierro que poseen un papel importante en diversos procesos fisiológicos, incluyendo a los transportadores *Yellow Strip-Like1* y *3* (*YSL1* y *3*); *YSL4, YSL6, PIC1* y *FRO7* involucrados en el movimiento intracelular de hierro a través del cloroplasto (Divol, *et al.,* 2013; Duy *et al.,*2007; Jeong *et al.,* 2007) y *Mitochondrial Iron Transporter1* o *MIT1* en mitocondrias (Bashir *et al.,* 2011). Por otro lado, también ha sido descrito el uso de citrato para movilizar hierro a través del floema (Curie *et al.,* 2009; Waters *et al.,* 2006) además de la existencia de una familia de péptidos con un motivo concenso de aminoácidos en el C-terminal llamados *IRON-MAN (IMA),* esenciales para la captura de hierro en plantas (Grillet *et al.,* 2018).

Después de la floración, las semillas dentro de los frutos acumulan nutrientes que serán utilizados durante la transición de metabolismo heterotrófico a autotrófico (REFERENCIA), es decir, antes de que las raíces sean competentes y la fotosíntesis se establezca. Se ha estudiado como el micronutriente Fe se acumula en las semillas. El desarrollo de técnicas que permiten visualizar el hierro ha permitido generar grandes avances en esta área. Utilizando un análisis de fluorescencia de rayos-X (XRF), se describió que en embriones silvestres de *Arabidopsis thaliana*, alrededor del 50% del hierro total se acumula alrededor de la provasculatura del embrión (Kim *et al.,* 2006; Schnell-Ramos *et al.,* 2013). Posteriormente, el desarrollo de una tinción histoquímica de Fe (de ahora en adelante Perls/DAB), permitió determinar por primera vez que el hierro

se acumula específicamente en las vacuolas de las células de la endodermis, un tipo celular que rodea la provasculatura (Roschzttardtz *et al.,* 2009). Cabe mencionar que la tinción Perls/DAB es un método rápido y simple de detección de Fe^{2+} y Fe^{3+}, y que permite obtener una mejor resolución a nivel subcelular (Roschzttardtz *et al.,* 2009).

Utilizando estrategias de genética reversa fue posible identificar a *Vacuolar Iron Transporter1* o *VIT1* como un gen clave involucrado en la distribución de Fe en embriones silvestres de Arabidopsis. Utilizando XRF y la tinción Perls/DAB fue posible determinar que en embriones mutantes *vit1* el hierro cambia su ubicación a las vacuolas de las células del cortex del embrión (Kim *et al.,* 2006; Roschzttardtz *et al.,* 2011). Es importante destacar que en estas mutantes no se ve afectado el contenido total de hierro acumulado en el embrión, sin embargo, en condiciones de déficit de hierro, mutantes *vit1* no son capaces de desarrollarse correctamente luego de la germinación, lo que sugiere que la acumulación de hierro en la endodermis es esencial para la sobrevivencia de las plántulas luego de germinar (Kim *et al.,* 2006). Por otro lado, recientemente se describió que el transportador *Metal Tolerance Protein8* (*MTP8*) es el responsable de la acumulación de hierro en las vacuolas de las células del cortex en mutantes *vit1.* Adicionalmente, en la doble mutante *vit1 mtp8* el hierro se acumula en todos los tipos celulares del embrión (Chu *et al.,* 2017). A la fecha, *VIT1* y *MTP8* son los únicos transportadores descritos involucrados en la distribución de Fe en el embrión de Arabidopsis.

Si bien la mayoría de los estudios de distribución de hierro en semillas se han realizado en Arabidopsis, utilizando arroz y trigo fue posible determinar que en Monocotiledóneas el escenario es completamente diferente. En este caso, la mayor

concentración de hierro se encuentra en la capa de la aleurona, mientras que la cantidad de hierro acumulada en el embrión y en el endosperma es muy baja (Takahashi *et al.,* 2009; Iwai *et al.,* 2012; De Brier *et al.,* 2016). Uno de nuestros principales objetivos como laboratorio es identificar los mecanismos que controlan la distribución y almacenamiento de Fe en semillas para el posterior desarrollo de estrategias de biofortificación. Una de las principales interrogantes que poseemos como grupo de investigación circula en torno a cómo es la distribución de hierro en semillas distintas a Arabidopsis.

Las semillas son de gran relevancia para los la nutrición de humanos. Entre un 30% y un 70% de la energía consumida a diario proviene de alimentos derivados de semillas (Graf *et al.,* 2015), por lo que fomentar el consumo de las semillas de diversos tipos de cereales y pseudo cereales representa una gran oportunidad para combatir diversos tipos de desordenes nutricionales a nivel mundial (Poutanen *et al.,* 2014). En este sentido, *Chenopodium quinoa* Willd o quinoa es un pseudo cereal con gran valor nutricional que durante siglos ha sido la base de la dienta de distintas culturas indígenas y que poco a poco ha ganado un papel importante en la dieta humana a nivel global (Jarvis *et al.,* 2016). Quinoa se caracteriza por estar adaptado a una gran variedad de ecosistemas, incluyendo el altiplano de la cordillera de los Andes (>3500m por sobre el nivel del mar), donde ha desarrollado tolerancia a distintos tipos de estrés abiótico (Aloisi *et al.* 2016).

En lo que respecta a hierro, la semilla de quinoa posee entre 3 y 5 veces más que la semilla de Arabidosis (Kim *et* al., *2006;* Valencia *et al.,* 1999). Hasta la fecha se desconoce donde se almacena el Fe en la semilla de quinoa, ni los ligandos utilizados para movilizar y almacenar este micronutriente. Cabe mencionar que las semillas de

quinoa son sustancialmente diferentes a las de Arabidopsis. A nivel general se pueden identificar tres tejidos diferentes: (1) el embrión, ubicado hacia la periferia de la semilla; (2) una o dos capas de endosperma que rodean el eje hipocotilo-radícula del embrión; (3) y el perisperma, ubicado en la zona central de la semilla (López-Fernández and Maldonado, 2013; Prego *et al.,* 1998); A diferencia de Arabidopsis, donde cerca del 95% del volumen total de la semilla es ocupado por el embrión, mientras que el 5% restante corresponde al endosperma.

A través de un análisis citoquímico y de ultraestructura fue posible determinar los principales componentes intracelulares almacenados en cada tejido de la semilla de quinoa. A nivel general, fue posible observar una gran cantidad de gránulos de almidón acumulados en el perisperma, mientras que vacuolas con cuerpos lipídico y cuerpos proteicos con estructuras de cristal tipo globoides, y una gran cantidad de proplastidios con depósitos de ferritinas son las principales estructuras identificadas tanto en el endosperma como en el embrión. Además, análisis por EDX a los cuerpos proteicos del endosperma y el embrión permitió determinar que las estructuras tipo globoide poseen grandes cantidades de potasio, magnesio y fósforo, sin embargo aún no ha sidO posible identificar la localización subcelular del hierro en estas semillas (Prego *et al.,* 1998).

Las ferritinas corresponden a una clase universal de proteínas multiméricas (conformadas por 24 sub-unidades) que se encuentran presente en todos los reinos de la vida, exceptuando en las levaduras, y que pueden almacenar entre 2.000 y 4.000 átomos de hierro en su cavidad central (Briat *et al.,* 2010; Ravet *et al.,* 2009). En animales ha sido ampliamente descrito que la función principal de estas proteínas en el almacenamiento de hierro y el suministro de metal para el metabolismo según sea

necesario (Theil, 2003). En plantas, el rol de las ferritinas aún no está por completo elucidado y la mayoría de las hipótesis existentes han sido formuladas basadas en la correlación entre la localización de estas proteínas y su expresión en respuesta a estímulos ambientales. A lo largo de su ciclo de vida, las plantas se enfrentan a diversos tipos de estreses los cuáles conllevan a un aumento de hierro libre intracelular lo que se traduce en la producción de especies reactivas de oxígeno (ROS). En Arabidopsis ha sido reportado que hay un aumento la expresión de los genes que codifican para ferritinas en respuesta a estrés, por lo que es muy posible que las ferritinas ayuden a la planta a sobrellevar estas situaciones adversas, modulando el contenido de hierro libre y de este modo evitando la producción de ROS (Ravet *et al.,* 2009).

Recientemente, en *Arabidopsis thaliana* la relevancia de las ferritinas como proteínas de almacenamiento de hierro durante el desarrollo de la semilla ha sido puesta en duda debido a la importancia que posee la remobilización vacuolar de Fe mediada por los transportadores NRAMP3 y 4 (Lanquar *et al.,* 2005). Arabidopsis posee cuatro genes que codifican para ferritinas (*AtFER1-4*), de los cuáles solo *AtFER2* se expresa en semillas, mientras que los otros tres se expresan en tejido vegetativo y reproductivo (Petit *et al.,* 2001). Plantas mutantes para el gen *AtFER2* no presentan ningún fenotipo macroscópico visible, mientras que la tasa de germinación, el contenido de hierro y el desarrollo de la planta post-germinación no se ven afectados al ser comparados con una planta silvestre, incluso en condiciones de déficit de hierro. Estas observaciones son consistentes con que la estimación de hierro asociada a ferritinas en semillas de Arabidopsis representa menos del 5% del contenido total de Fe en la semilla (Ravet *et al.,* 2009).

En lo que respecta a quinoa, no se conoce la función molecular que poseen las ferritinas en semillas, sin embargo, la gran cantidad de hierro acumulado en las semillas, el hecho de que las vacuolas del embrión de quinoa no acumulen grandes cantidades de hierro, junto a la presencia de ferritinas tanto en el embrión como en el endosperma abren nuevas preguntas respecto a los mecanismos moleculares que controlan el transporte, distribución y acumulación de hierro en esta planta.

HIPÓTESIS

Chenopodium quinoa posee un mecanismo de acumulación de hierro diferente al de Arabidopsis que involucra ferritinas.

OBJETIVO GENERAL

Determinar el mecanismo de acumulación de hierro durante la maduración de la semilla de *Chenopodium quinoa*.

OBJETIVOS ESPECÍFICOS

1. Generar un modelo evolutivamente cercano a *Arabidopsis thaliana* que permita comparar la distribución de hierro durante el desarrollo de la semilla de *Chenopodium quinoa.*
2. Determinar la localización sub-celular y el estadio de desarrollo donde comienza a acumularse las reservas de hierro en el embrión de *Chenopodium quinoa.*
3. Determinar la acumulación de ferritinas en el embrión de *Chenopodium quinoa.*

RESULTADOS

Capítulo 1: Dynamic subcellular localization of iron during embryo development in Brassicaceae seeds

Ibeas M.A.[1], Grant-Grant S.[1] Navarro N.[1], Perez M.F.[2], Roschzttardtz H.[1]*

[1] Departamento de Genética Molecular y Microbiología. Pontificia Universidad Católica de Chile. [2] Departamento de Ecología, Pontificia Universidad Católica de Chile.

Abstract

Iron is an essential micronutrient for plants. Little is know about how iron is loaded in embryo during seed development. In this article we used Perls/DAB staining in order to reveal iron localization at the cellular and subcellular levels in different Brassicaceae seed species. In dry seeds of *Brassica napus, Nasturtium officinale, Lepidium sativum, Camelina sativa and Brassica oleracea* iron localizes in vacuoles of cells surrounding provasculature in cotyledons and hypocotyl. Using *B. napus* and *N. officinale* as model plants we determined where iron localizes during seed development. Our results indicate that iron is not detectable by Perls/DAB staining in heart stage embryo cells. Interestingly, at torpedo development stage iron localizes in nuclei of different cells type, including integument, free cell endosperm and almost all embryo cells. Later, iron is detected in cytoplasmic structures in different embryo cell types. Our results indicate that iron accumulates in nuclei in specific stages of embryo maturation before to be localized in vacuoles of cells surrounding provasculature in mature seeds.

Introduction

Nutrient reserves in the seed must be sufficient to sustain plant establishment until the root system has developed enough to provide nutrients from the soils. High nutrient content of seeds is particularly important for plants growing in unfavorable nutritional conditions and has been related to higher seed viability and seedling vigor. Besides its impact on plant growth, nutrient levels in seeds are an important consideration for human and/or livestock seed-based nutrition (Roschzttardtz et al., 2017).

Iron is an essential micronutrient for plant growth and development. Despite its importance, the prevalent low iron bioavailability in the soils of main agricultural areas of the world limits plant productivity, fertility, and germination rates (Guerinot and Yi, 1994). As a consequence, iron contents in seeds is diminished which results in negative impacts in human and animal health, since seeds are a main source of food for humans and animals (Fan et al., 2008; DeFries et al., 2015). In humans, iron deficiency in women and children under two years is a serious and growing public health problem and a major concern for the World Health Organization. Therefore, understanding seed iron distribution and storage at the physiological and molecular level is key to design biotechnological applications to improve iron content of staple seeds.

Different approaches have been used in order to study where iron localizes in plant organs and at subcellular level. In plant, iron accumulates in different compartments depending of the tissue and cell type. Among these are apoplast in root vasculature, plastids in leaves and pollen grain, vacuoles in embryos, and nuclei in different cell types

(Lanquar et al., 2005; Roschzttardtz et al., 2009; Roschzttardtz et al., 2011; Roschzttardtz et al., 2013).

Regarding seeds, it has been described that iron accumulates in embryo during maturation stage of seed development (Roschzttardtz et al., 2009). So far, VACUOLAR IRON TRANSPORTER1 (VIT1) is the only player described involved in the iron loading into the vacuoles of endodermis cell layer in Arabidopsis embryos. Mutants in *VIT1* mislocalize iron, which accumulates in vacuoles of cortex cells in hypocotyl and subepidermal cells of abaxial side of cotyledons (Kim et al., 2006; Roschzttardtz et al., 2009; Eroglu et al., 2017). Interestingly, *vit1* mutants do not grow correctly in iron deficient conditions, suggesting that iron localization in seed has an important role in seed physiology. In the absence of functional VIT1 or during germination, the manganese and iron transporter MTP8 is responsible for loading iron in the vacuoles of subepidermal cells of cotyledons (Eroglu et al., 2017).

Little is known about the mechanism involved in iron loading in embryo during seed development. Recently Grillet et al., (2014) described that ascorbate efflux from Pea embryos is required for iron loading in seeds.

In this article we used, as model plants, species belonging to the Brassicaceae family in order to describe the subcellular compartments where iron accumulates in embryo during seed development. One of our models, *Brassica napus* L., is one of the most important oil crops almost all over the world. The tetraploid *B. napus* is a hybrid derived from *Brassica oleracea* and *Brassica rapa* and it shares more than 86% similarity in protein coding sequence with *A. thaliana* (Cavell et al., 1998; Parkin et al., 2005). Furthermore,

rapseed is not only important for vegetal oil, but also a major source for industrial materials such as biofuel (Chen et al., 2017).

Our results show that iron is accumulated first in nuclei of integument cells, endosperm and embryo cells in the early maturation stage of seed development before being located in vacuoles of endodermis cells. Some differences in iron localization were also observed in mature embryos of *Brassica napus*, *Nasturtium officinale*, *Lepidium sativum*, *Brassica oleracea* and *Camelina sativa* compared with *Arabidopsis thaliana*.

Materials and Methods

Plant material and growth conditions

Brassica napus, Nasturtium officinale, Camelina sativa, *Lepidium sativum* and *Brassica oleracea* seeds were purchased at a local market. *B. napus* and *N. officinale* plants were grown on soil in a greenhouse at 23ºC under long-day conditions (16-h/8-h day/night cycle).

Histochemical staining of iron with the Perls/DAB procedure

Iron staining was performed according to Roschzttardtz et al., (2009). *Brassica napus, Nasturtium officinale, Camelina sativa, Brassica oleracea* and *Lepidium sativum* dry seeds or seeds from *B. Napus* and *N. officinale* at different developmental stage were

vacuum infiltrated with fixation solution (2% w/v paraformaldehyde in 1 mM phosphate buffer pH 7.0) for 45 min and incubated for 16 h in the same solution. The fixated seeds were dehydrated with ascendant concentration of ethanol (50%, 70%, 80%, 90%, 95% and 100%), later were incubated 12 h with a solution of butanol/ethanol 1:1 (v/v), and finally were incubated 12 h with 100% butanol. Then, the seeds were embedded in the Technovit 7100 resin (Kulzer) according to the manufacturer's instructions and thin sections (3 µm) were cut and were deposited on glass slides. For Perls/DAB staining, slides were incubated with 2% (v/v) HCl and 2% (w/v) K-ferrocyanide (Sigma Aldrich) for 45 minutes For the DAB intensification, each glass slide was washed with distilled water, later were incubated in a methanol solution containing 0.01 M NaN_3 (Sigma Aldrich) and 0,3% (v/v) H_2O_2 (Merck) for 1 hour, and then washed with 0.1 M phosphate buffer (pH 7.4). For the intensification reaction, the glass slides were incubated between 10 and 30 minutes in a 0.1 M phosphate buffer (pH 7.4) solution containing 0.025% (v/v) H_2O_2, and 0.005% (w/v) $CoCl_2*6H_2O$ (intensification solution). To stop the reaction each slide was rinsed with distilled water.

Iron quantification

A microwave-assisted acid digestion was performed using 6.0 mL of concentrated HNO_3 (Winkler) and 1.0 mL of 30% (v/v) H_2O_2 added over 10 to 20 mg of seeds of each genotype. The colorless digestate were filled up to 15 mL using deionized water. The iron content of each genotype was measured in triplicate using inductively coupled plasma mass spectrometry (ICP-MS).

Microscopy and staining with DAPI, Perls/DAB and Toluidine blue

Thin sections were first stained with DAPI in order to visualize nuclei (Roschzttardtz et al., 2013), the same section was stained by Perls/DAB, as described above. Then were stained with toluidine blue. Each slide was incubated in a 0.5% (w/v) solution of toluidine blue for 2 min and rinsed with distilled water. The samples were observed and photographed with a Nikon Eclipse 80i microscope.

Results

Iron concentration and distribution in dry seeds of close related species to *Arabidopsis thaliana*

To evaluate iron concentration and distribution in dry seeds from closely related Arabidopsis species, first we determine iron content in dry seeds from *Arabidopsis thaliana, Brassica napus* and *Nasturtium officinale* (Figure 1A). Dry seeds were isolated, and a microwave-assisted acid digestion was performed. Figure 1B show iron concentration of each species determined by inductively coupled plasma mass spectrometry (ICP-MS). Iron concentration in *Arabidopsis thaliana* and *Brassica napus* dry seeds (70,4 and 64,6 µg of iron/g of seeds, respectively) was lower compared to *Nasturtium officinale* (116,6 µg of iron/g of seeds), suggesting that there is no relation between iron concentration and seed size, as *Brassica napus* have the biggest seeds (Figure 1A) but also have a similar iron content as *Arabidopsis thaliana*.

In order to determine where iron localizes in dry seed embryos from species closely related to Arabidopsis thaliana, we analyzed seven different plant species: *Brassica napus, Nasturtium officinale, Camelina sativa*, *Arabidopsis thaliana*, *Lepidium sativum, Brassica oleracea and Brassica oleracea* var. capitate (Figure 2 and Figure S2). Embryos from dry seeds were isolated and fixed. Thin sections of different embryo regions were analyzed, in particular, cotyledon and hypocotyl. Figure 2 and Supplemental Figure 2 show Perls/DAB staining revealing iron distribution in embryos from these species. Cotyledons accumulate iron in vacuoles of cells surrounding provasculature (Figure 2A to 2D, Figure S2A and S2B) as has been described before for *Arabidopsis thaliana* (Roschzttardtz et al., 2009). Provasculature complexity in cotyledon is clearly higher than Arabidopsis (Roschzttardtz et al., 2014; Roschzttardtz et al., 2017). Iron accumulation was not observed in other cell types like protodermis and cortex cells in dry seed embryos (Figure 2A to 2D, Figure S2A and S2B).

Interestingly, transversal sections of hypocotyl show differences in the number of cell layer where iron accumulates compared to Arabidopsis hypocotyl, where only one cell layer accumulates iron (Roschzttardtz et al., 2009). We found that at least two-cell layers accumulate iron in the hypocotyl of *Brassica napus, Nasturtium officinale, Camelina sativa, Lepidium sativum* and *Brassica oleracea* dry seed embryos (Figure 2E to 2G, Figure S2C and S2D, respectively). Despite the differences in the number of cell layers where iron accumulates in dry seeds of *Brassica napus, Nasturtium officinale, Camelina sativa, Lepidium sativum* and *Brassica oleracea* compared to *Arabidopsis thaliana*, at subcellular level iron is stored in the vacuoles in cells surrounding provasculature (Figure 2A to 2D, Figure S2A and S2B).

Analyses of embryonic root tips indicate that iron accumulates in different cells identified as endodermis-cortex cells (Figure S3).

Figure S1 shows the phylogenetic tree of the 5 species of Brassicaceae family used in this study. Interestingly, iron localization in vacuoles is a conserved trait in the analyzed plant species. As indicated above, differences were only observed in the number of cell layers that accumulate iron in the hypocotyls.

Iron distribution during *Brassica napus* seed development

As we showed, iron accumulates in vacuoles in embryos of seven species of Brassicaceae (Figure 2 and Figure S2). We used *Brassica napus* plants as model to study where iron localizes during seed development. *B. napus* produces bigger seeds compared with Arabidopsis plants allowing to study with more details different seed regions during its development (Figure 1A). In a phylogenetic point of view, *B. napus* is the more distant specie to *A. thaliana* used in this study. The fact that iron localizes in vacuoles of mature *B. napus* seeds is a strong indication that it is a conserved trait. Using *A. thaliana* as plant model it has been described that iron accumulates in embryo during seed maturation stages (Roschzttardtz et al., 2009), for this reason we analyzed three different stages of seed maturation, torpedo, bend cotyledon and mature stage before seed desiccation. In order to describe seed structures where iron accumulates before to be loaded into the embryo, we used in our analysis whole seeds including seed coat,

endosperm and embryo. Whole seeds of *B. napus* containing embryos in different maturation stages as indicated above, were fixed and embedded in Technovit resin according to Material and Methods.

The analysis of seeds with torpedo embryo stages revealed that iron localizes mainly in nuclei of integument cells, free cell endosperm and in different cell layers in the embryo (Figure 3). At this embryo stage, Perls/DAB and Toluidine blue staining show that in protodermal, cortex, endodermis and provasculature cells iron is localized in nuclei (Figure 3A and 3B). As vacuoles look empty after both staining, our results suggest that vacuoles of embryo cells are not an important compartment for iron storage at this developmental stage. Interestingly, strong iron staining was observed in nuclei (one to three iron pools were observed) of the free cell endosperm surrounding the embryo (Figure 3C and 3D).

Later, in seeds containing bend cotyledon embryo stage, integuments no longer contain iron inside the nuclei (Figure 4A and 4B). In the embryo, the number of cells containing iron in nuclei decreases. In embryonic root tips and cotyledons, iron is localized in structures surrounding the nuclei (Figure 4A, 4B, 4E and 4F), while vacuoles are starting to load iron in the hypocotyl endodermis cell layer (Figure 4C and 4D).

In mature seeds before desiccation, iron does not localize in nuclei (Figure 5) and vacuoles are the principal compartments for iron storage (Figure 5B and 5D). At this late stage of seed development, cells adjacent to provasculature load iron and protodermis and cortex cells have not detectable iron as the previous seed developmental stages (Figure 5).

In order to determine whether iron is accumulated in nuclei before torpedo stages, we use *N. officinale* developing embryos. Our results indicate that in the heart stage of embryo development iron is not detectable by Perls/DAB staining in embryo cells. This result strongly supports the conclusion that iron localizes in nuclei of embryo cells in the torpedo stage (Figure S5). Similar stages of seed maturation were analyzed using *N. officinale*. No differences in iron distribution were observed compared to *B. napus* (Figure S4).

Iron distribution at subcellular level during seed maturation

In order to confirm the subcellular compartments accumulating iron during development we performed consecutively staining with DAPI, Perls/DAB and toluidine blue on the same sections of different developmental stages of *B. napus* embryos. Iron accumulates in nuclei of different cell types in early maturation stages of seed development (Figure 6A to E). In bend cotyledon stage, iron is not longer detected in nuclei and accumulates in cytoplasmic structures (Figure 6K to O). Finally in mature stages, vacuoles of cells surrounding provasculature start to accumulate iron (Figure 6P to T). Details of unique cells are shown in Figure 6, indicating unambiguously were iron localizes in different cases, nuclei, cytoplasmic structures or vacuoles.

Discussion

During seed development embryo accumulates nutrients that will be used in the transition of heterotrophy to autotrophy metabolism during germination and post germination stage of development. In the case of iron, the principal transporter expressed in root involved in iron acquisition in Arabidopsis *IRT1* is expressed 3-4 days after germination (Lanquar et al., 2005). Before roots are able to acquire iron from the soil, iron that was stored during seed development is remobilized from vacuoles of endodermis and bundle sheath cells (Lanquar et al., 2005; Roschzttardtz et al., 2009, Mary et al., 2015). When iron is not correctly localized as in *vit1* mutants or not remobilized as in *nramp3 nramp4* double mutant, germinated seeds have difficulties to growth in iron deficiency conditions (Kim et al., 2006; Lanquar et al., 2005; Mary et al., 2015). This indicates that iron storage and localization in embryos is pivotal for seed physiology (Kim et al., 2006).

In this article, different stages of seed maturation were analyzed by a histochemical approach (Perls/DAB staining) in order to reveal iron localization. Perls/DAB method is specific and very sensitive for iron detection and can detect both Fe^{2+} and Fe^{3+} forms (Roschzttardtz et al., 2009). Other methods more quantitative have been used to reveal iron localization in seeds, indicating that an Arabidopsis embryo contains a fraction of the total iron of a seed (Schnell Ramos, 2013). Despite of not being a quantitative method, Perls/DAB staining allows to obtain information at subcellular level of any plant tissues and stages of plant development (Roschzttardtz et al., 2013).

Our analysis showed that iron was not localized in an unique subcellular compartment during seed development. In early maturation stages (embryo in torpedo stage) iron was localized principally in nuclei of integument, endosperm and embryo cells. This result is very surprising, indicating that vacuoles are not the only relevant subcellular compartment for iron storage during seed development (Figure 3 and 4). Interestingly, Perls/DAB did not detect iron in embryo at heart stage, suggesting strongly that iron is accumulated in nuclei not before torpedo stages (Figure S5). Later iron seems to be gradually concentrated in structures surrounding nuclei (possibly mitochondria or endoplasmic reticulum) before to be loaded into the vacuoles of endodermis cells (Figure 5). The micronutrient manganese has been detected in endoplasmic reticulum during seed development, but more studies may be performed in order to identify the nature of the structures where iron is detected before to be mobilized to the vacuoles (Otegui et al., 2002). A model of iron dynamic during embryo loading is shown in figure 7. The presence of iron in nuclei of pea embryos was previously reported in Roschzttardtz et al., (2011), however, in this present study we shown that iron localizes in nuclei only during torpedo stages in Brassicaceae seeds. These results open interesting questions about the role of nuclei at this embryo stage of development. Our results suggest that nuclei may be a reservoir of iron during seed development or that iron may have unknown functions in nuclei of embryos in torpedo stage. Very recently, a specific role of iron in promoting meristematic cell division in adventitious root formation has been proposed (Hilo et al., 2017), however, the molecular role of iron in nuclei remains unknown.

Regarding iron distribution, we found that species closely related to *Arabidopsis thaliana* have some differences in dry seed embryos. For instance, iron is accumulated into the

vacuoles of two-cell layer in mature embryos of *Lepidium sativum* showing a clear difference with Arabidopsis mature embryos, where only one cell layer accumulates iron (Figure 2; Roschzttardtz et al., 2009). A study reporting iron localization in dry seeds of 13 genoypes of three Phaseolus species has shown that large concentrations of iron are accumulated in the cytoplasm of cells surrounding the provascular bundles (Cvitanich et al., 2010). In the case of monocots, the highest iron concentration occurs in scutellum and outer regions of the embryo while a very low Fe is detected in the outermost layers of the endosperm and the single-layered aleurone that surrounds the endosperm (Johnson et al., 2011). This suggests that different mechanisms of iron acquisition may play important roles in different seed species. In our group, we are interested in elucidating the molecular mechanisms that may explain these differences.

Acknowledgements

The authors are greatly indebted to Xavier Jordana and María Isabel Gómez for their continued support and encouragement. This work was funded by FONDECYT 1160334 (Chilean Government) and INTER 6809 (Pontificia Universidad Católica de Chile-VRI) to HR, and Millennium Nucleus Center for Plant Systems and Synthetic Biology (NC130030). PhD students work was supported by Conicyt-Chile grants 21160350 (to MAI) and 21170951 (to SG).

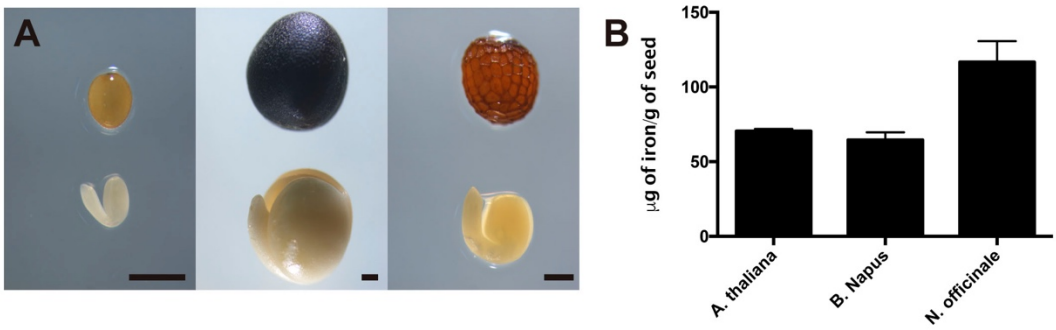

Figure 1. Iron concentration in Brassicaceae seeds. **A.** Differences in size and form of Brassicales mature seeds and embryos used in this study. The left panel shows *Arabidopsis thaliana*, the middle panel shows *Brassica napus* and the right panel shows *Nasturtium officinale*. The bar scale represents 500 µm. **B.** Iron concentration in mature seeds determined by ICP-MS. Values are the mean of three biological replicates (±SD).

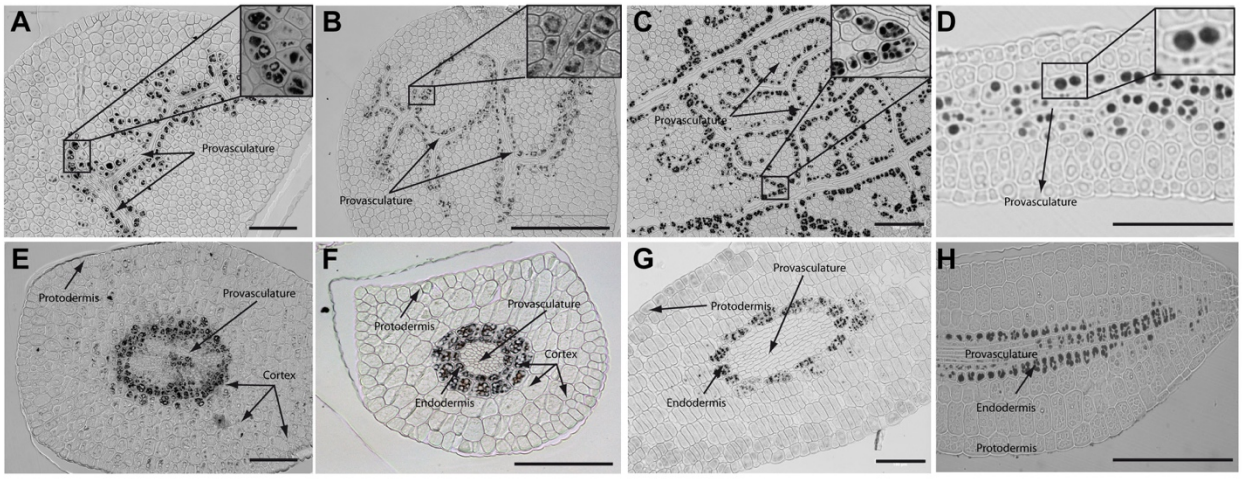

Figure 2. Iron distribution in *Brassica napus, Nasturtium officinale, Camelina sativa* and *Arabidopsis thaliana* dry seed embryos. Embryos were dissected from dry seeds and thin sections were obtained and stained with Perls/DAB in order to reveal iron accumulation. *Brassica napus* sections are shown in A, and E; *Nasturtium officinale* sections are shown in B and F; *Camelina sativa* sections are shown in C and G and *Arabidopsis thaliana* sections are shown in D and H panels. Cotyledons and hypocotyl are shown in A to D and E to H respectively. In panel A to D a zoom is shown in order to indicate iron accumulation into the vacuoles. Bars in panels correspond to 100 μm.

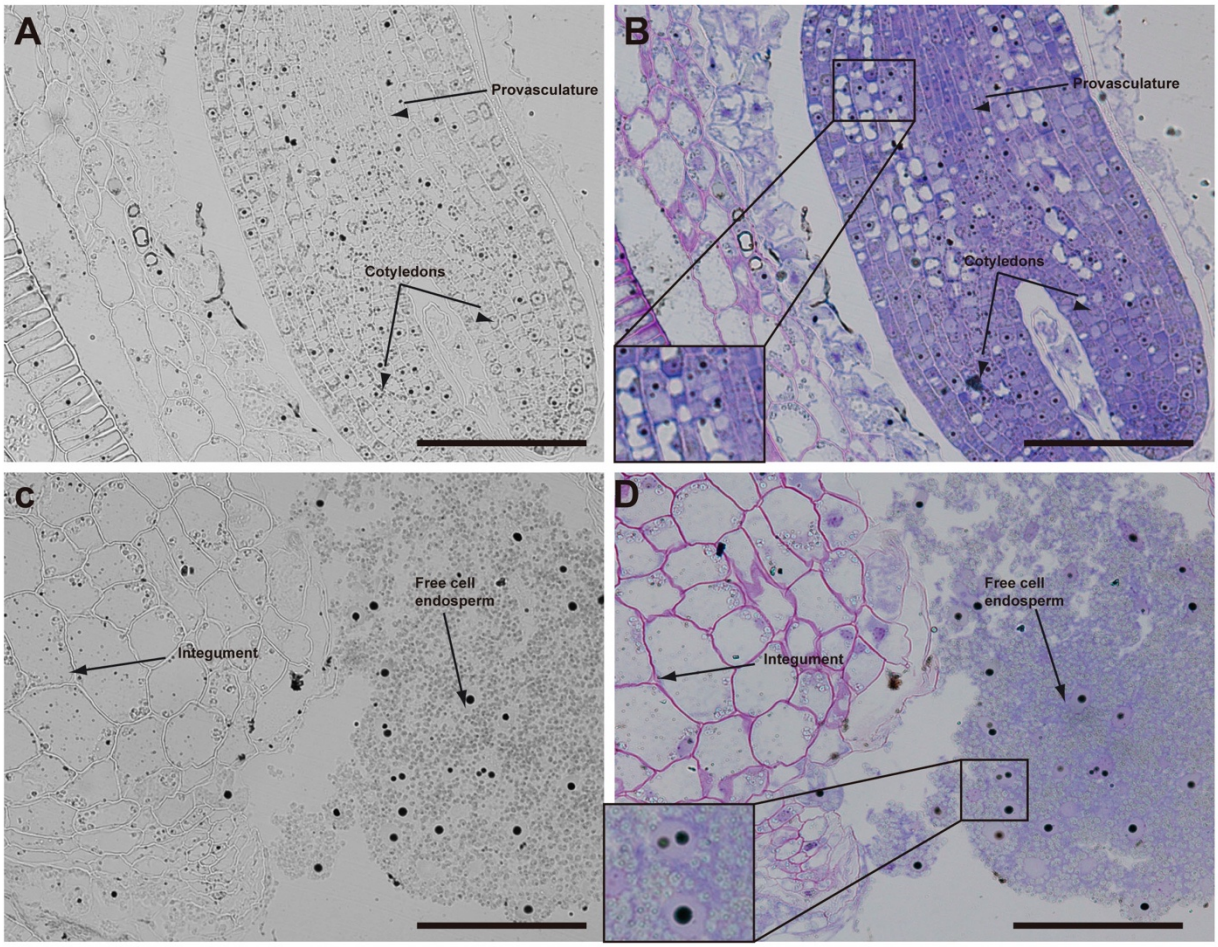

Figure 3. Iron distribution in *Brassica napus* seeds in torpedo embryo stage. *Brassica napus* seeds at torpedo stage dissected from siliques were embedded in Technovit resin and sectioned (3 µm) and then stained with Perls/DAB (A-D) and then with Toluidine blue (B and D). In panel B and D a zoom is shown in order to indicate iron accumulation into the nuclei of the cells (B) and free cell endosperm (D). The scale bar represents 100 µm

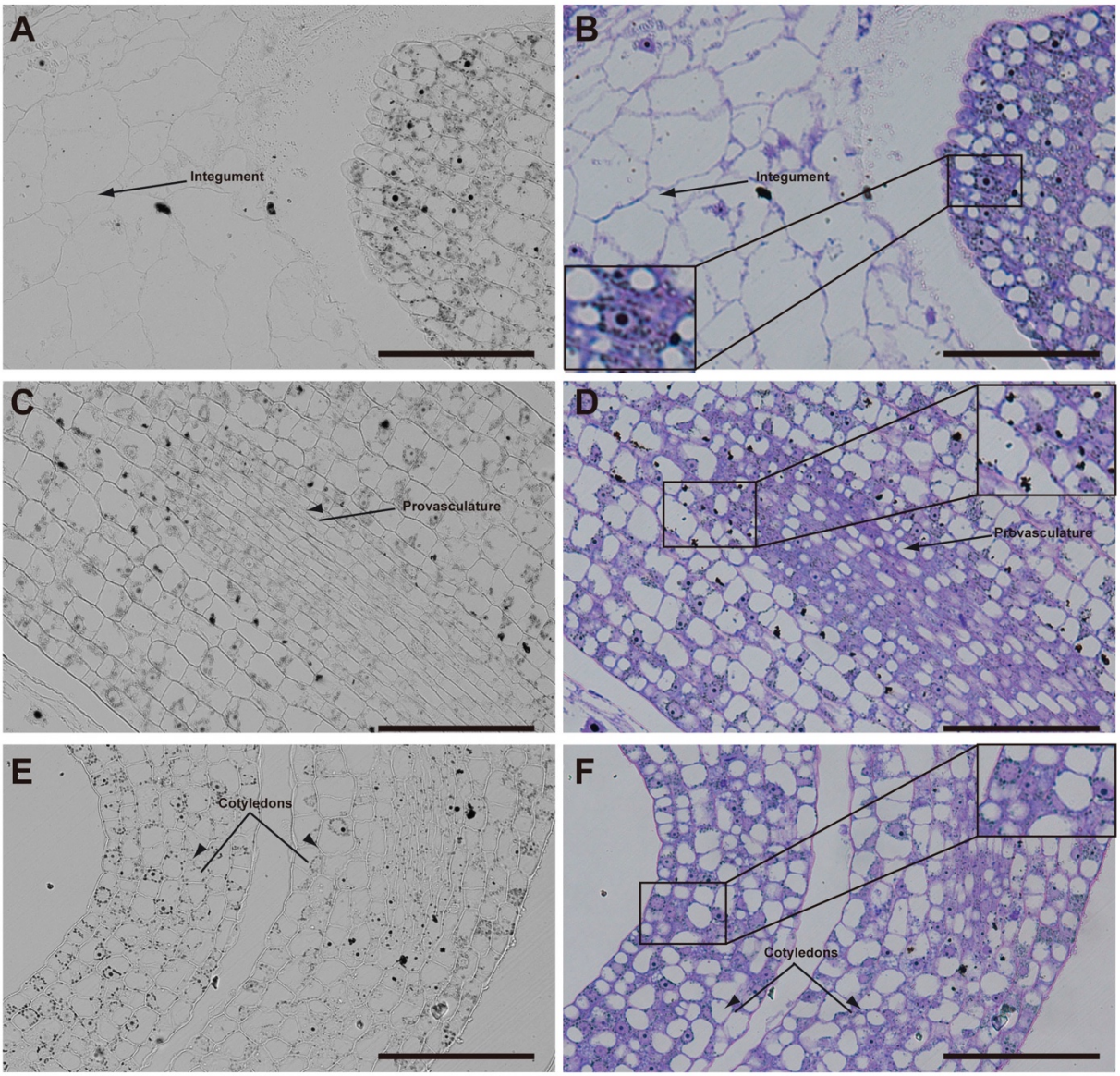

Figure 4. Iron distribution in *Brassica napus* seeds in bend cotyledon embryo stage. *Brassica napus* seeds at the bend cotyledon stage dissected from siliques were embedded in Technovit resin and sectioned (3 µm) and stained with Perls/DAB (A-F) and then with Toluidine blue (D-F). In panel D to F a zoom is shown in order to indicate iron accumulation into and around the nuclei (B), cellular structures surrounding the nuclei (B and F) and iron accumulation inside vacuoles (D). The scale bar represents 100 µm.

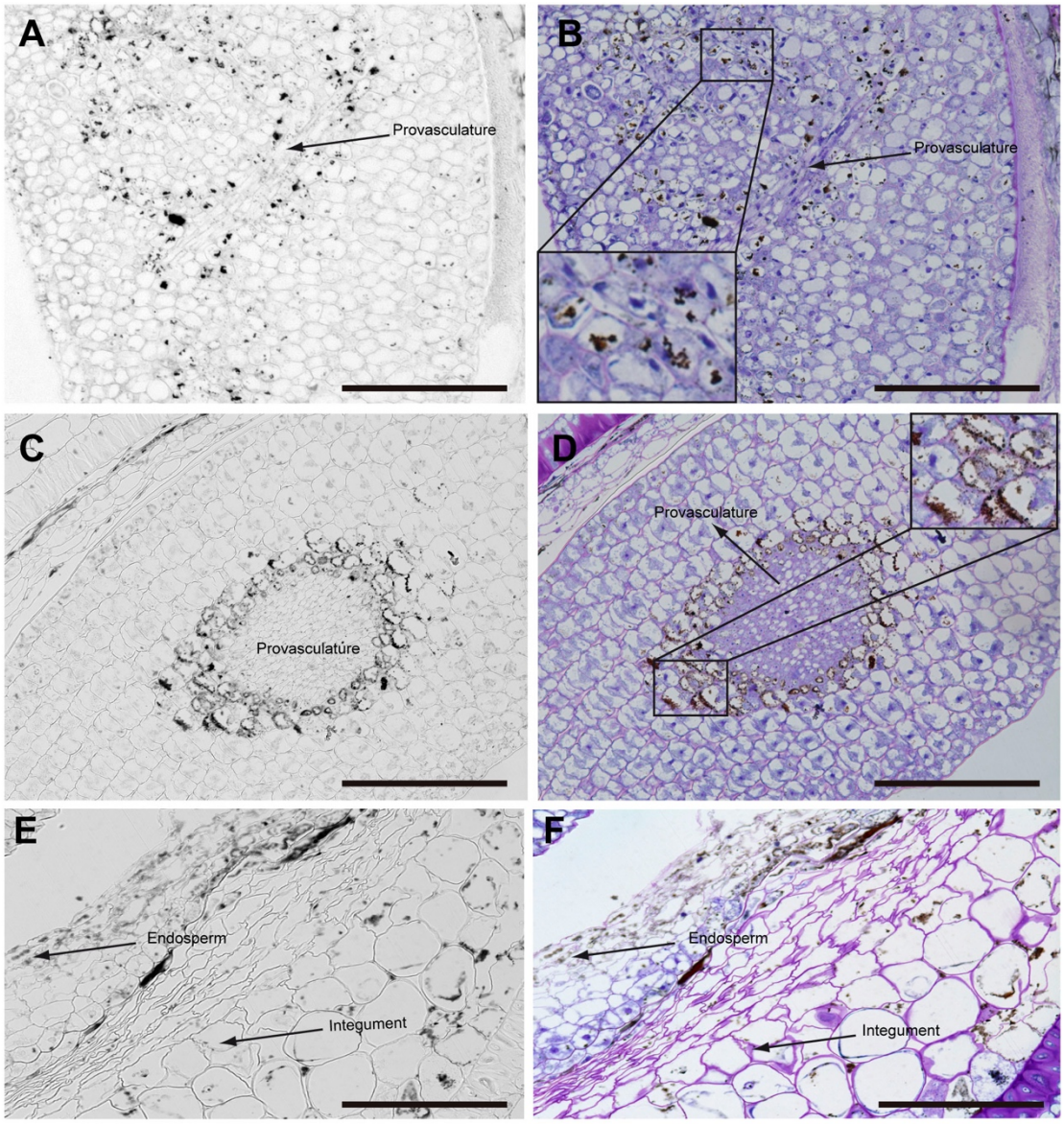

Figure 5. Iron distribution in *Brassica napus* seeds in mature embryo stage before seed desiccation. *Brassica napus* seeds at the mature embryo before seed desiccation stage dissected from siliques were embedded in Technovit resin and sectioned (3 µm) and stained with Perls/DAB (A-F) and then with Toluidine blue (B, D and F). Cotyledons, hypocotyl and endosperm-seed coat are shown in A-B, C-D and E-F, respectively. In panel B and D a zoom are shown in order to indicate iron accumulation in the vacuoles. The scale bar represents 100 µm.

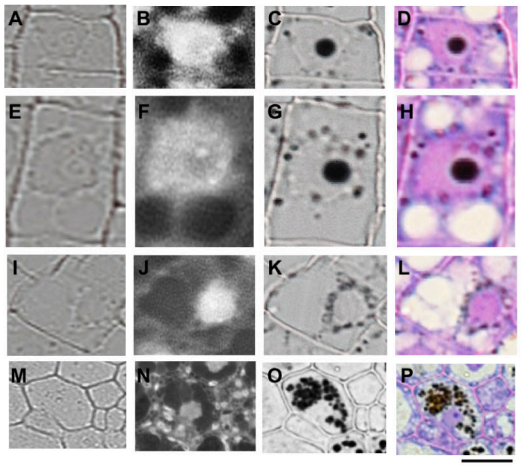

Figure 6. Iron transit across different subcellular compartments during seed development. Iron accumulates in nuclei of different cell type in early maturation stages of seed development (A to E). In bend cotyledon stage, iron is detected in nuclei and cytoplasmic structures (F to J), later is not longer detected in nuclei but accumulates only in cytoplasmic structures (K to O), and finally in mature stages vacuoles of cells surrounding provasculature start to accumulate iron (P to T). DAPI staining was used in order to visualize nuclei (B, G, L and Q). Perls/DAB staining was used to reveal iron pools inside the cells (C, H, M and R). Merge between DAPI and Perls/DAB staining are shown in D, I, N and S and Toluidine blue staining was used to reveal different cell structures (E, J, O and T). A, F, K and P show controls cells without staining. The subsequent staining was performed over the same sections. The scale bar represents 20 μm.

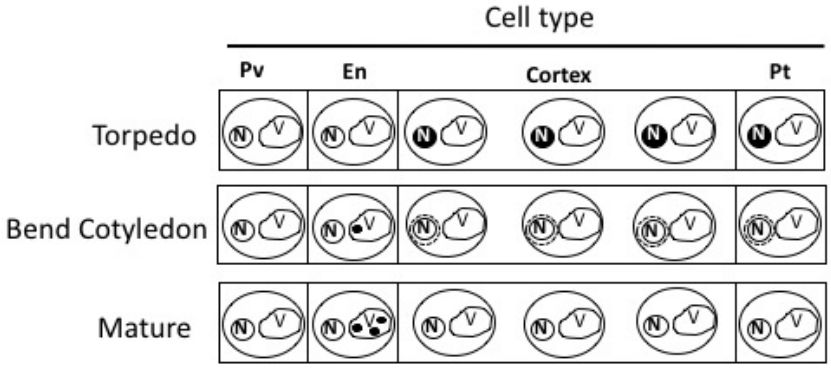

Figure 7. Model of iron distribution during seed development. At the torpedo stage iron accumulates mainly in nuclei of different cell types. In bend cotyledon stage, iron is not longer detected in nuclei and accumulates in unknown cytoplasmic structures (possibly endoplasmic reticulum or mitochondria), later in mature stages vacuoles of cells surrounding provasculature start to accumulate iron. Pv: provasculature; En: Endodermis; Pt: Protodermis. N: Nuclei; V. Vacuole.

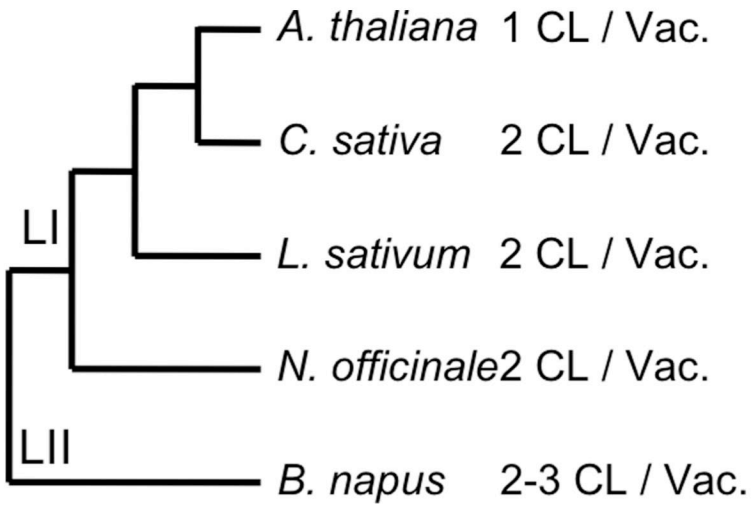

Figure S1. Number of cell layers and cellular compartment that storage iron in the hypocotyl embryo of five Brassicaceae species mapped on the phylogenetic tree of the family obtained with complete plastomes (modified from Guo et al., 2017). LI and LII are the lineages I and II described for Brassicaceae family. CL: Cell layer; Vac: Vacuole.

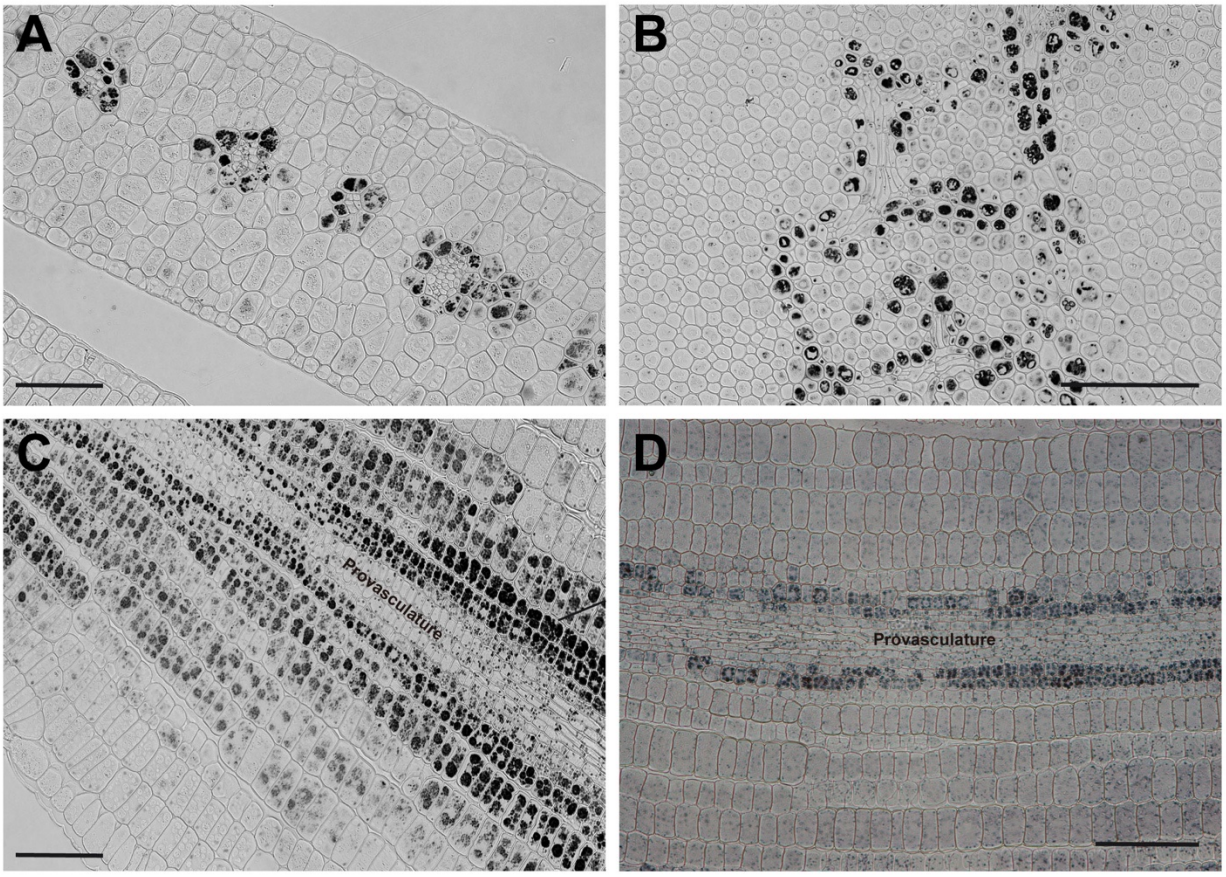

Figure S2. Iron distribution in dry seed embryos of *Brassica oleracea* and ***Lepidium sativum*.** Embryos were dissected from dry seeds and thin sections were obtained and stained with Perls/DAB in order to reveal iron accumulation. Cotyledon transversal sections and hypocotyl longitudinal sections are shown for *Brassica oleracea* (A and C); cotyledon longitudinal section is shown for *Brassica oleracea* var. capitate (B) and hypocotyl longitudinal section is shown for *Lepidium sativum* (D). Bars in panels correspond to 100 μm.

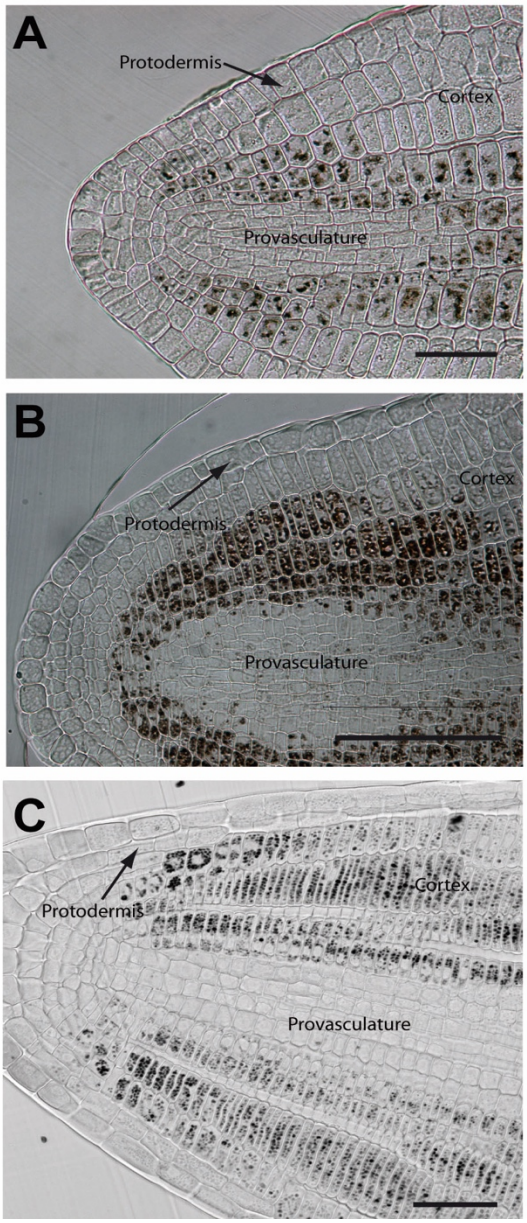

Figure S3. Iron distribution in *Brassica napus*, *Nasturtium officinale* and *Camelina sativa* roots tips embryo. Embryos were dissected from dry seeds and thin sections were obtained and stained with Perls/DAB in order to reveal iron accumulation. *Brassica napus, Nasturtium officinale and Camelina sativa* root tip sections are shown in A-C panels, respectively. Bars in panels correspond to 100 µm.

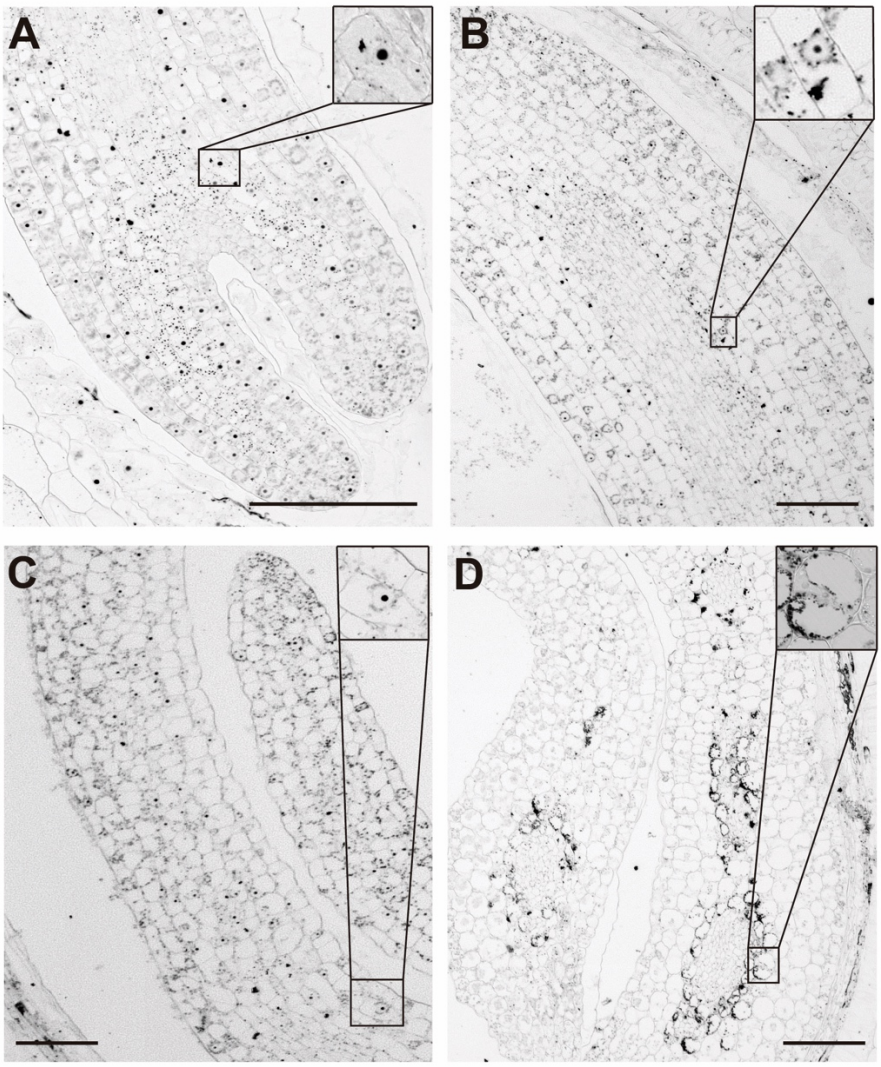

Figure S4. Iron distribution during *Nasturtium officinale* seed development. Embryos were dissected from seeds at different developmental stages and thin sections were obtained and stained with Perls/DAB in order to determine iron accumulation. A, Torpedo stage is shown; B and C, Hypocotyl and cotyledon from bend cotyledon stage are shown; D, Cotyledons from mature embryo before desiccation are shown. A zoom is shown in order to indicate iron accumulation at subcellular level. The scale bar represents 100 µm.

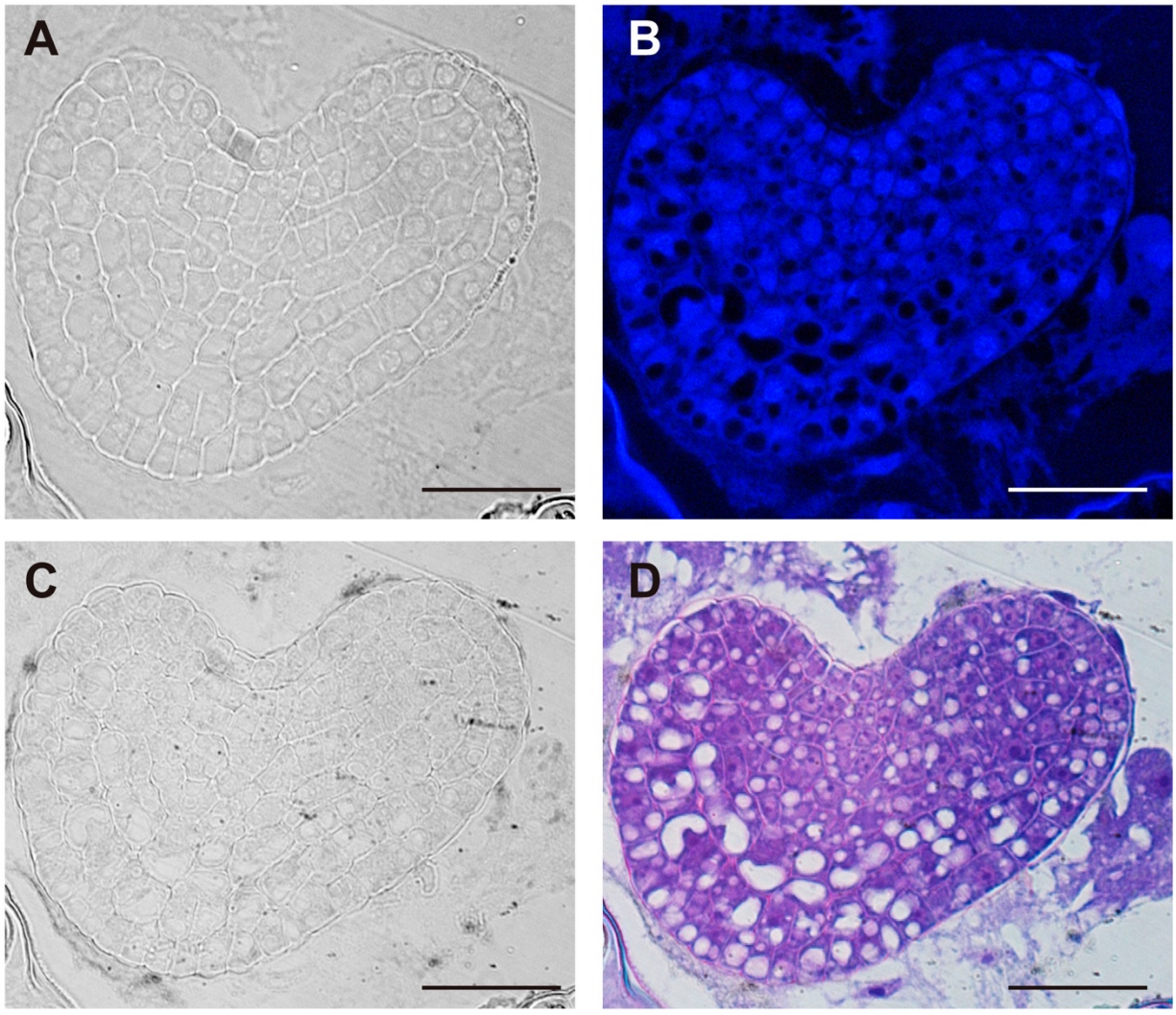

Figure S5. Iron distribution in *Nasturtium officinale* at heart stage. Embryos were dissected from seeds at heart stage and thin sections were obtained and stained with Perls/DAB in order to reveal iron accumulation. A, Control of Perls/DAB staining; B, DAPI staining visualized by UV light; C, Perls/DAB staining; and D, Toluidine blue staining. The scale bar represents 100 µm.

Capítulo 2: The diverse iron distribution in Eudicotyledoneae seeds: from Arabidopsis to Quinoa.

Ibeas M.A.[1], Grant-Grant S.[1], Coronas M.F.[1], Vargas-Pérez J.[1], Navarro N.[1], Abreu I.[2], Castillo-Michel H.[3], Avalos-Cembrano N.[1], Paez-Valencia J.[4], Pérez F.[5], González-Guerrero M.[4], Roschzttardtz H.[1]*

[1]Facultad de Ciencias Biológicas. Pontificia Universidad Católica de Chile, Chile.

[2]Centro de Biotecnología y Genómica de Plantas (UPM-INIA), Universidad Politécnica de Madrid, Spain.

[3]ID21, European Synchrotron Radiation Facility (ESRF), Grenoble, France.

[4]University of Wisconsin-Madison, WI, USA.

[5]Departamento de Ecología, Pontificia Universidad Católica de Chile, Chile.

*Corresponding author: Hannetz Roschzttardtz

Email: hroschzttardtz@bio.puc.cl

Running Title: Apomorphic Iron distribution in seed plant model

Abstract

Seeds accumulate iron during embryo maturation stages of embryogenesis. Using *Arabidopsis thaliana* as model plant, it has been described that mature embryos accumulate iron within a specific cell layer, the endodermis. This distribution pattern was conserved in most of the analyzed members from Brassicales, with the exception of the basal *Vasconcellea pubescens* that also showed elevated amounts of iron in cortex cells. To determine whether the *V. pubescens* iron distribution was indicative of a wider pattern in non-Brassicales Eudicotyledoneae, we studied iron distribution pattern in different embryos belonging to plant species from different Orders from Eudicotyledoneae and one basal from Magnoliidae. The results obtained indicate that iron distribution in *A. thaliana* embryo is an extreme case of apomorphic character found in Brassicales, not-extensive to the rest of Eudicotyledoneae.

Key words: Apomorphy, Arabidopsis, Quinoa, embryo, iron, phylogeny.

Introduction

Increased iron content in seeds is an important agronomic trait. This is due to the relevance of this element in seed production (Marschner, 2005; Roschzttardtz et al., 2011), embryo development, and seedling germination and growth (Kim et al., 2003; Lanquar et al., 2005), as well as in human nutrition (Murgia et al., 2012). In spite of this essential role, the prevalent low iron bioavailability in the soil of most of the main agricultural areas of the world, limits plant productivity, fertility, and even germination rates (Guerinot and Yi, 1994). Consequently, a substantial effort has been dedicated to unravelling the molecular bases controlling iron homeostasis, how plants incorporate and distribute iron throughout their organs, and how iron is stored in the seeds (Walker and Waters, 2011; Kobayashi and Nishizawa, 2012; Grillet et al., 2014; Flis et al., 2016; Tsai and Schmidt, 2017).

Iron distribution in seeds has been studied in monocots and Eudicotyledoneae. Using rice and wheat as models it was concluded that most of the iron in monocot plants is stored in the aleurone layer (Iwai et al., 2012; de Brier et al., 2016). In Eudicotyledoneae, the majority of work has been carried out in Arabidopsis. It has been estimated that approximately 50% of the seed iron content is stored in endodermal cells (Schnell-Ramos et al., 2013; Roschzttardtz et al., 2009). Results from experiments using multiple iron-imaging methods showed that the vast majority of the seed embryo iron is located in vacuoles (Kim et al., 2006; Schnell-Ramos et al., 2013; Roschzttardtz et al., 2009). This is in contrast to other plant tissues in which iron has also been detected in plastids, associated with ferritin, and in nucleoli (Roschzttardtz et al., 2013; Roschzttardtz et al., 2011).

Iron accumulates steadily in the endodermal vacuole during the maturation stage of embryo development, and is subsequently used during postgerminative growth (Lanquar et al., 2005; Roschzttardtz et al., 2009). The defects shown by the *vit1* and *nramp3 nramp4* mutants under iron deficiency conditions suggest that proper iron storage seems essential for seed germination and post-germinative growth (Lanquar et al., 2005; Kim et al., 2006; Mary et al., 2015). These mutant plants are defective in iron loading into the vacuoles of endodermal cells during embryo maturation, a process mediated by the transporter AtVIT1 (VACUOLAR IRON TRANSPORTER1) (Kim et al., 2006); or in iron recovery from vacuoles in these cells via the AtNRAMP3 and AtNRAMP4 (NATURAL RESISTANCE ASSOCIATED MACROPHAGE PROTEIN3 and 4) transporters during germination (Lanquar et al., 2005).

Closely related Brassicaceae embryos accumulate iron very similarly to Arabidopsis, *i.e.* in vacuoles of cells surrounding the embryo provasculature (Ibeas et al., 2017). However, reports on another Eudicotyledoneae, the legume *Phaseolus vulgaris*, showed broader iron localization. While iron hotspots were detected in cotyledons in a pattern resembling the provasculature, the metal was also evenly distributed in the rest of the organ (Cvitanich et al., 2010). This alternative way of accumulating iron in the seed could indicate that the storage of this nutrient in Eudicotyledoneae is more diverse than what has been reported to date. Considering the importance of Eudicotyledoneae as crops, and the need to improve the iron content in the edible parts (DeFries et al., 2015), we set to study iron distribution in embryos from a wide range of orders belonging to dicotyledonous plants. Our results show that the iron distribution pattern in the Arabidopsis embryo is not extended to all Eudicotyledoneae, it rather seems to be a

derived character only observed in the Brassicaceae family. We also found that Caryophyllales has a distinct iron distribution pattern and that iron loading during *C. quinoa* seed development is different than what we had previously observed in Brassicaceae (Ibeas et al., 2017), suggesting there might be different strategies for the storage of iron in these seeds.

Material and Methods

Plant material and growth conditions

Most of the seeds used in this study were purchased at a local market or harvested in public gardens. Some seeds were collected in the field and identified before being deposited in the herbarium at the Departamento de Ecología, Pontificia Universidad Católica de Chile. The list of species used in this study is in Table S1. *Chenopodium quinoa* plants were grown on soil in a greenhouse at 23ºC under long-day condition (16-h/8-h day/night cycle).

Histochemical staining of iron with Perls/DAB method

Seed embryos from the species indicated in Table S1 or *Chenopodium quinoa* seeds at different developmental stages were isolated and fixed with 2% w/v paraformaldehyde in

1 mM phosphate buffer pH 7.0 for 45 min. The following steps were performed according to Roschzttardtz et al., (2009) and Ibeas et al., (2017).

Synchrotron µ-XRF

Quinoa seeds were embedded in OCT (Optimal Cutting Temperature) resin and plunge-frozen in isopentane chilled in liquid nitrogen. Longitudinal sections (30 µm) were prepared using a cryomicrotome (Leica, RM2265-LN22) at -50°C and immediately imaged at beamline ID21 at the ESRF (European Synchrotron Radiation Facility, Grenoble, France). Elemental distribution was mapped by micro X-ray fluorescence (µXRF) under cryogenic conditions (Cotte et al. 2017). The beam was focused with the use of KB mirrors to a size of 0.5 × 0.9 μm^2 (V×H). The fluorescence signal was detected using an 80mm^2 active area SGX Si drift detector with a Be window. Two photodiodes were used to measure the incident and transmitted beam intensities. Scans were acquired with an energy of 7.2 keV (Fe k-edge) with a dwell time of 100 ms per pixel, and a pixel size of 2 µm x 2 µm. RGB color maps and Fe, Mn and P elemental maps were created using PyMca software (Solé et al. 2007).

Phylogenetic analysis

A phylogenetic tree of the species in the data set was assembled using the phylogeny of angiosperms at family level, from the Angiosperm Phylogeny Group (APG IV, 2016). To resolve relationships within Brassicaceae we followed Guo et al., (2017), which uses 77

protein coding regions. Branch lengths were set to 1.0. Species were assigned to four categories according to Fe location in seed embryos: endodermis; inner layers of cortex, external cortex or protodermis. Ancestral states of iron location were reconstructed using Mesquite (Maddison and Maddison, 2004) based on one-parameter model.

Results

Differences in iron distribution in embryos of the order Brassicales

Analyses on species from the Brassicaceae family showed that their embryos have similar subcellular iron distribution in cotyledons and hypocotyl (Ibeas et al., 2017). In *Arabidopsis thaliana*, *Camelina sativa, Nasturtium officinale, Lepidium sativum* and *Brassica napus* dry seed embryos*,* iron accumulates in the vacuoles of cells surrounding the provasculature. Some differences in the number of cells that store iron were observed in the hypocotyl: while Arabidopsis only presented a one cell layer, the other species have two or more (Roschzttardtz et al., 2009; Ibeas et al., 2017).

We extended this study to members of other families within the Brassicales order. We performed Perls/DAB staining on *Cleome hassleriana* (Cleomaceae Family) and *Capparis spinosa* (Capparaceae Family). Embryo sections revealed that iron accumulates in cells that surround the provasculature in a similar manner as embryos from Brassicaceae species (Figure 1). Some differences were observed in *Capparis spinosa*, where a group of cells between provasculature regions in cotyledons showed

iron accumulation in vacuoles (Figure S1). Surprisingly, when analyzing the member of the Caricaceae family *Vasconcellea pubescens* (a more ancestral Brassicales), we observed that several cortex cells accumulate iron. This pattern sets it apart from the rest of Brassicales embryos studied to date and suggests that Brassicaceae embryo cortex cells may also accumulate iron (Figure 1).

Iron distribution in embryos from different orders of Eudicotyledoneae

To inquire whether the observation that *V. pubescencs* has a differential iron distribution is an exception or an ancestral trait lost at some point in the Brassicales order, Perls/DAB analyses were carried out in embryos from six representative Eudicotyledoneae Orders (Sapindales, Rosales, Zygophyllales, Solanales, Asterales, Caryophyllales) and one basal specie from Magnoliidae (Magnoliales). Interestingly, the analysis of embryos from those orders showed that iron accumulates in several cell layers including endodermis and cortex cells. In some cases, iron was also detected in the protodermis (Solanales, Asterales and Magnoliales; Figure 2). These results indicate that the Arabidopsis embryo has an uncommon iron distribution compared to embryos of seed plants from other Orders of the Eudicotyledoneae class. Moreover, a more detailed analysis of *P. chilensis* Perls/DAB-stained section shows that iron also seems to accumulate extracellularly, in what might be described as the cortex apoplast (Figure 2).

Iron distribution in Caryophyllales embryos

In order to evaluate iron distribution in species from other orders, seed embryos of several species belonging to Caryophyllales were used to determine whether iron distribution might differ within the same order. Figure 3A shows embryos from *Fagopyrum esculentum*, *Chenopodium quinoa* and *Phytolacca dioica.* In all cases, embryos were isolated and fixed, and then thin sections were analyzed, in particular hypocotyl and cotyledon. Using Perls/DAB staining we found that in all the species analyzed, iron was present in several embryo cell types, including endodermis and cortex cells. This result indicates that this pattern of iron distribution is conserved within this order (Figure 3A). We also analyzed embryos from *Spinacia oleracea, Beta vulgaris,* and *Rheum rhabarbarum* (Figure 7).

Next, we used synchrotron-based micro X-ray fluorescence (SμXRF) to independently confirm iron distribution using Perls/DAB staining in *Chenopodium quinoa* seeds. Dry seeds were sectioned and analyzed by S-μXRF, showing iron accumulation in several cell layers in hypocotyl but excluding provasculature (Figure 3B). S-μXRF also showed Mn accumulation in several cell layers of *C. quinoa* hypocotyl (probably cortex) in contrast with the restricted localization of Mn in the subepidermal layer of plant model *Arabidopsis thaliana* (Kim et al., 2006; Punshon et al., 2012; Schnell Ramos et al., 2013; Eroglu et al., 2017).

Iron distribution during *Chenopodium quinoa* seed development

Previously, our group reported for the first time that some Brassicaceae species accumulate iron in two embryo cell types (endodermis and one cell layer of cortex). We

also showed that in early stages of *B. napus* seed development, iron accumulates in nuclei of the free cell endosperm and in all embryo cell types. Later, iron is relocated to cytoplasmic structures, and finally, at the mature stage, iron is accumulated in vacuoles of the endodermis and cortex (Ibeas et al, 2017).

Because the iron distribution pattern in Caryophyllales is different from the pattern described above, we used *Chenopodium quinoa* as a model to study iron localization during seed development. *C. quinoa* is an emerging crop that has potential health benefits and an exceptional nutritional value. We analyzed four different stages of seed maturation in *Chenopodium quinoa*: early stages (between 3 and 7 days post anthesis), an intermediate stage (14 days post anthesis/cotyledon stage) and a late stage (21 days post anthesis/mature stage). In order to describe the seed structures where iron accumulates before being loaded into the embryo, we used whole seeds including seed coat, perisperm and embryo in our analyses.

Analysis of seed sections containing early embryo developmental stages revealed that there are no detectable iron pools in seed coat, perisperm or embryos (Figure 4). In seeds containing embryos at the cotyledon stage iron is detected inside the nuclei and in structures surrounding the nuclei (Figure 5B). Interestingly, longitudinal sections of the entire seed showed detectable iron pools in the integuments. Strong iron staining was observed in cytoplasmic structures (Figure 5D). In order to confirm the subcellular compartments that accumulate iron we performed Perls/DAB and Toluidine blue staining on the same sections. The zoom of specific cells in Figure 5B and D, show that iron localizes in nuclei and cytoplasmic structures in the embryo. Moreover, there is strong iron staining in cytoplasmic structures in the integuments.

In mature seeds, iron is no longer localized in nuclei (Figure 6). At this stage, iron is detected in several embryonic cell types, including endodermis and cortex cells of cotyledons and hypocotyl (Figure 6B and D). Perls/DAB and Toluidine blue staining show that iron pools do not localize in nuclei in cotyledon and hypocotyl cells (Zoom in Figure 6B and D).

Discussion

Dietary iron deficiency is a major issue for human health, affecting more than 2 billion people around the world (Murgia et al., 2015). Seeds are a pivotal source of iron for humans and animals (Roschzttardtz et al., 2017). Therefore, understanding the molecular mechanisms involved in iron loading and distribution in seeds is critical for the development of biotechnological approaches to improve seed iron content. Generation of biofortified crops could be a financially sound strategy to deliver nutrients to the population, as an alternative to the continuous governmental investment in fortification and supplementation programs (DeFries et al., 2015). Thus, genetic biofortification of staple crops could result in an environmentally friendly and cost-effective strategy for the improvement of nutritional health (Guerinot and Yi, 1994).

Pioneer studies, using SμXRF and a histochemical method for iron detection in plant tissues (Perls/DAB stain), showed that iron accumulates in the vacuoles of the endodermis cell layer of *A. thaliana* mature embryos (Kim et al., 2006; Roschzttardtz et al., 2009; Eroglu et al., 2017; Ibeas et al., 2017). While this distribution pattern is conserved in the rest of the Brassicaceae family (Ibeas et al., 2017), it is not present in

legumes (Cvitanich et al., 2010). These observations suggest that embryos may have multiple ways to store iron. Consequently, by exploring this diversity, we should be able to propose suitable models to dissect the molecular mechanisms of seed iron storage and eventually translate these findings to crops of commercial and nutritional value. Towards this end, we used Perls/DAB staining to determine iron distribution in several plant species along the Eudicotyledoneae phylogeny. As a result, we obtained the first phylogenetic study of iron distribution in plant seed embryos. The results indicate that seed embryos belonging to different Eudicotyledoneae orders accumulate iron in several cell layers, with more diversity that what can be inferred by simply using Arabidopsis as model. In particular, cortex cells accumulate iron in all the embryo species analyzed except for Brassicales families Capparaceae, Cleomaceae and Brassicaceae. These results strongly suggest that iron distribution in cortex cells in embryos from Eudicotyledoneae embryo plants is a conserved characteristic from a phylogenetic point of view. We used S-μXRF as a second and independent method to confirm that in quinoa embryos, iron accumulates in several cell layers including the cortex and endodermis cells (Figure 3B).

Quinoa seed has high nutritional value and has recently started to be used as a novel functional food (Abugoch, 2009). This plant contains 15 mg of iron per 100 g of seeds, covering the daily iron needs of infants and adults (Konishi et al., 2004; National Academy Press, 2001). We evaluated iron accumulation during *Chenopodium quinoa* seed development and found that it does not accumulate iron in any seed tissue during the early developmental stages (Figure 4). This is in contrast with what was previously described for *B. napus* seeds, in which strong iron staining was observed in the nuclei of

the free cell endosperm surrounding the embryo, and also in several cell layers of the embryo at the torpedo stage (Ibeas et al*.,* 2017). This discovery opens new questions on the mechanisms of iron distribution and accumulation in these seeds, and will be used as the basis for the development of biotechnological strategies to increase total iron content in seeds for human consumption.

A side finding of this work is the broad distribution of Mn in the embryo of *C. quinoa* hypocotyl (Figure 3B), compared to the restricted location of Mn in the hypocotyl subepidermal tissue of *Arabidopsis thaliana* embryos (Kim et al., 2006; Punshon et al., 2012; Schnell Ramos et al., 2013; Eroglu et al., 2017). It has recently been shown that mutations in the genes *cax1cax3* (Punshon et al., 2012), *mtp8* and *vit1* (Eroglu et al., 2017) cause a broad distribution of Mn indicating that they are responsible for this localization. As proposed for iron, this finding will open new strategies for the development of Mn fortified seeds.

In addition to Brassicales, our analyses also showed that at least some Zygophyllales, such as *P. chilensis*, also have an unusual iron distribution. In this case, iron is distributed inside and outside the cells (apoplast). This iron pool would necessarily be accumulated in a different manner from the vacuolar-located. For instance, there would be no need for particular metal transporters as is the case for Arabidopsis (Kim et al., 2006; Lanquar et al., 2005). It would also be interesting to determine the iron ligands, and how assimilable it is. Further analyses of this and other Zygophyllales species will be carried out to ascertain the extension of this phenotype and to determine its molecular bases.

Regarding the widespread use of Arabidopsis as a Eudicotyledoneae model plant for iron nutrition, our results show that iron distribution in Arabidopsis embryos is not a widely conserved character in Eudicotyledoneae seed embryos and it corresponds to an apomorphic character. Ancestral reconstruction of the phylogeny of angiosperms with Maximum Parsimony or Maximum Likelihood indicated that the embryo of the ancestor of Brassicales, and probably of all Eudicotyledoneae, accumulates iron in several layers of the cortex (Figure 7). The loss of iron in the outer layers of the cortex evolved in the core of Brassicales, whereas the ability to accumulate iron only in endodermis is a derived trait of Arabidopsis. According to Beilstein et al. (2010), the apomorphy described in our study emerged between 120-70 Mya. In our opinion, Brassicales seeds could be used to evaluate molecular mechanisms involved in iron accumulation in the cortex cells, using information obtained from other species described in this article.

These results also open new questions on the mechanisms involved in iron accumulation and remobilization in cortex and protodermis cells, during embryogenesis and seed germination, respectively. From an evolutionary point of view, it will be interesting to study which competitive advantage determined the selection of this iron distribution in Brassicales species.

Acknowledgements

The authors are greatly indebted to Dr. Juan Keymer for his continued support and encouragement. *Vasconcellea pubescens seeds* were kindly provided by Dr. Maria José Letelier and Dr. Sebastián Godoy. This work was funded by FONDECYT 1160334

(Chilean Government) to HR. PhD students' work was supported by Conicyt-Chile grants 21160350 (to MAI), 21170951 (to SG) and 21151344 (to JVP).

Author Contribution

MAI, SG, JVP, NN, HR performed embryo dissections and Perls/DAB staining. IA, HCM, MGG, performed the SμXRF analysis. FP performed the phylogenetic analysis. All authors participated in the writing of the manuscript.

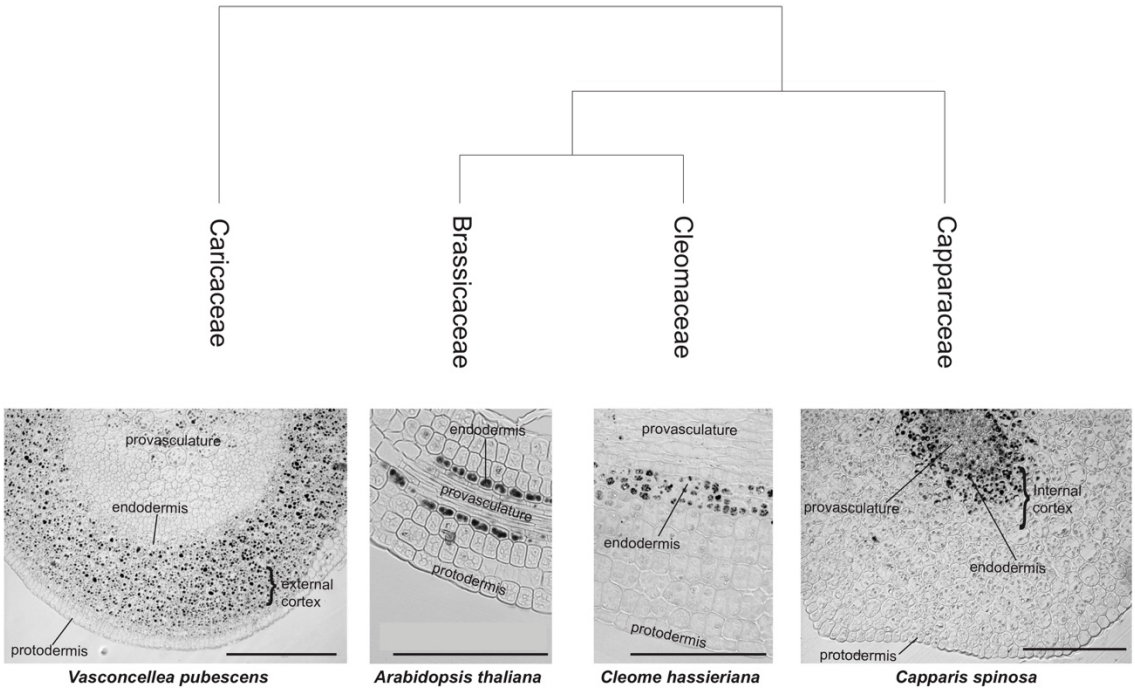

Figure 1. Iron distribution in Brassicales embryos. Iron distribution in hypocotyls of four Brassicales species were mapped on the phylogenetic tree modified from Hall et al., 2004. The analysis of sections using Perls/DAB of Brassicaceae family species was previously described in Ibeas et al. (2017). Iron is accumulated, in addition to endodermis, in the cortex cells (internal cortex, close to endodermis, and close to the protodermis, external cortex). A section of *A. thaliana* hypocotyl stained with Perls/DAB is shown. Bars in panels correspond to 100 μm.

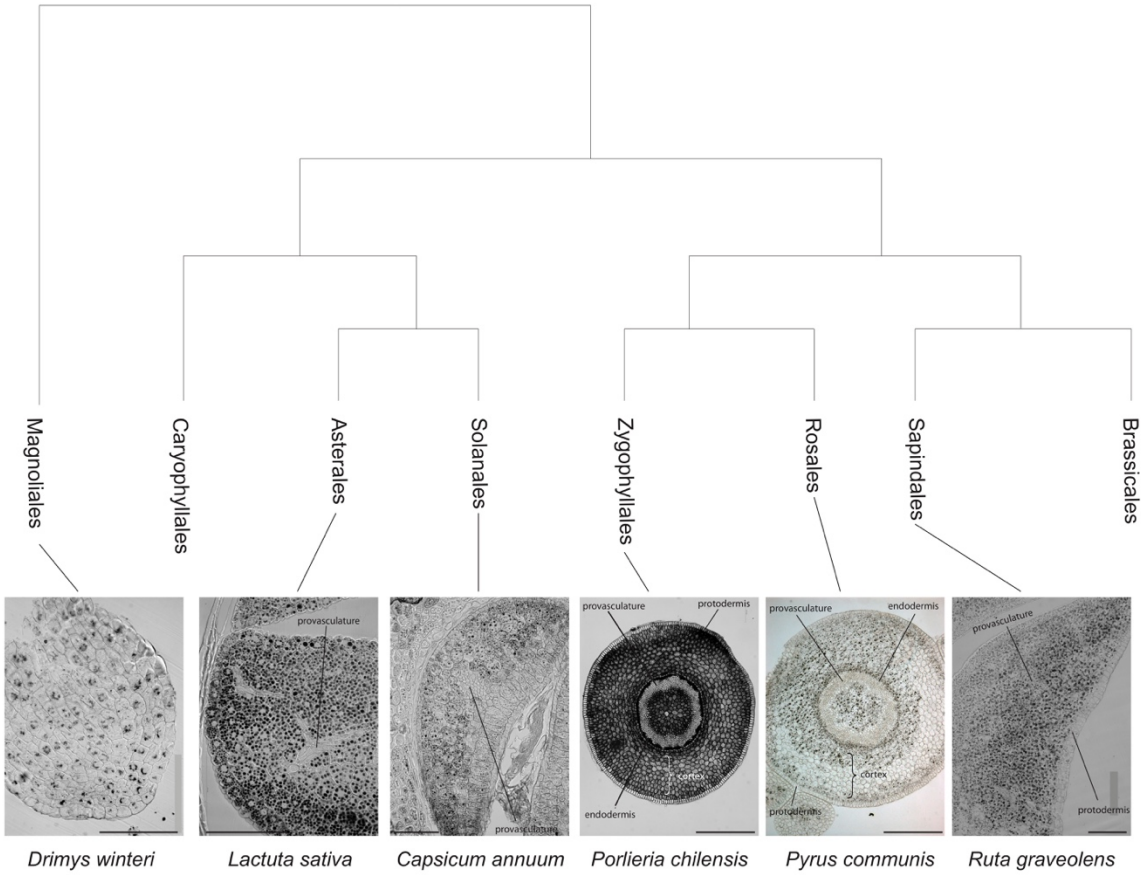

Figure 2. Iron distribution in Eudicotyledoneae mature embryos. Iron distribution was revealed by Perls/DAB staining of hypocotyls (*Porlieria chilensis* and *Pyrus communis*) or cotyledons sections (*Ruta graveolens*, *Capsicum annuum* and *Lactuca sativa*). The phylogenetic tree was assembled from APG IV (2016). Bars in panels correspond to 100 µm.

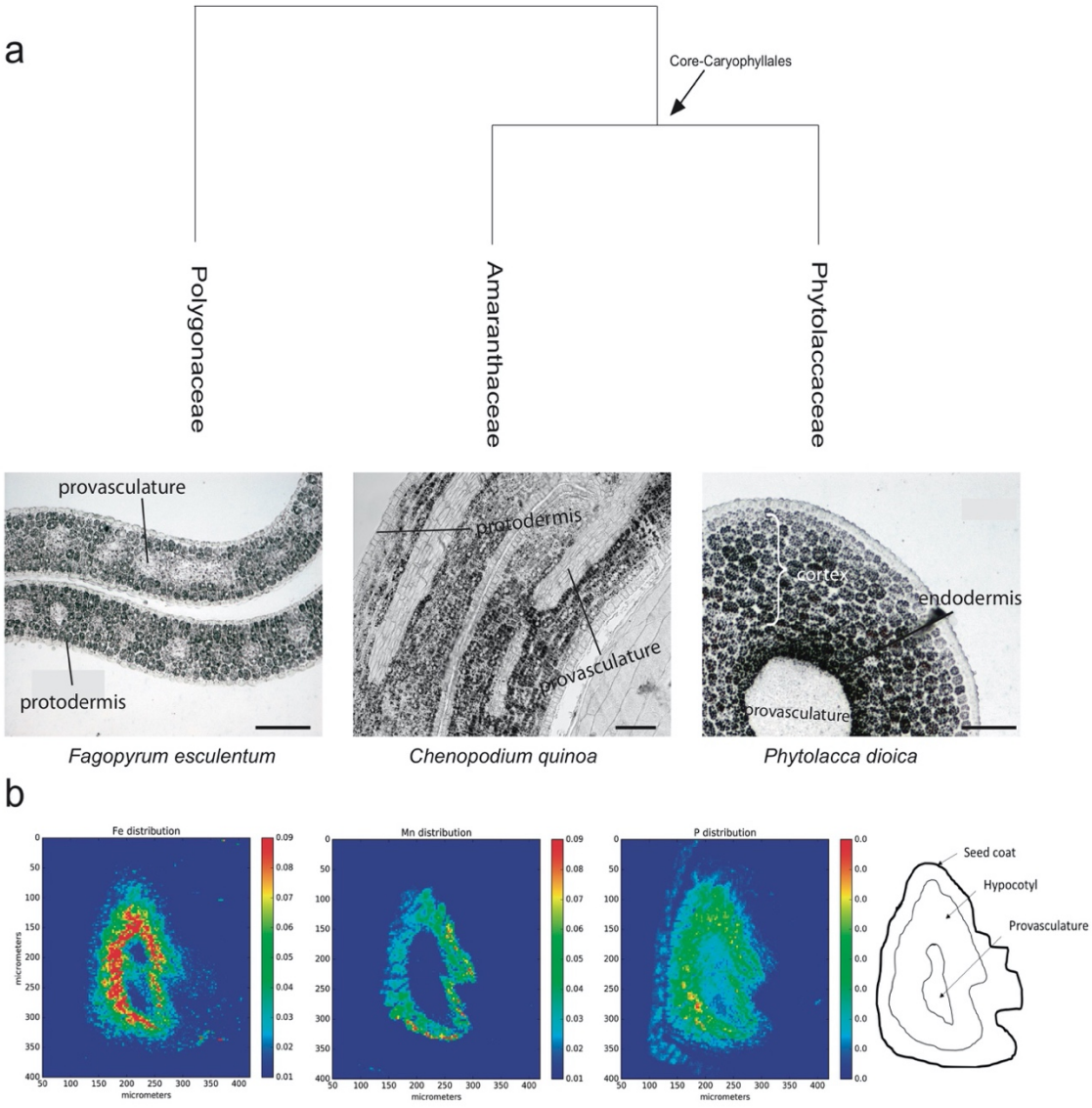

Figure 3. a) Iron distribution in Caryophyllales mature embryos. Perls/DAB stained embryo sections from polygonaceae, amaranthaceae and phytolaccaceae families (*Fagopyrum esculentum*, *Chenopodium quinoa* and *Phytolacca dioica*, respectively). Bars in panels correspond to 50 µm. b) Iron detection in hypocotyl Quinoa dry seed section using synchrotron-based micro X-ray fluorescence (SµXRF). P, Mn and Fe distribution are shown.

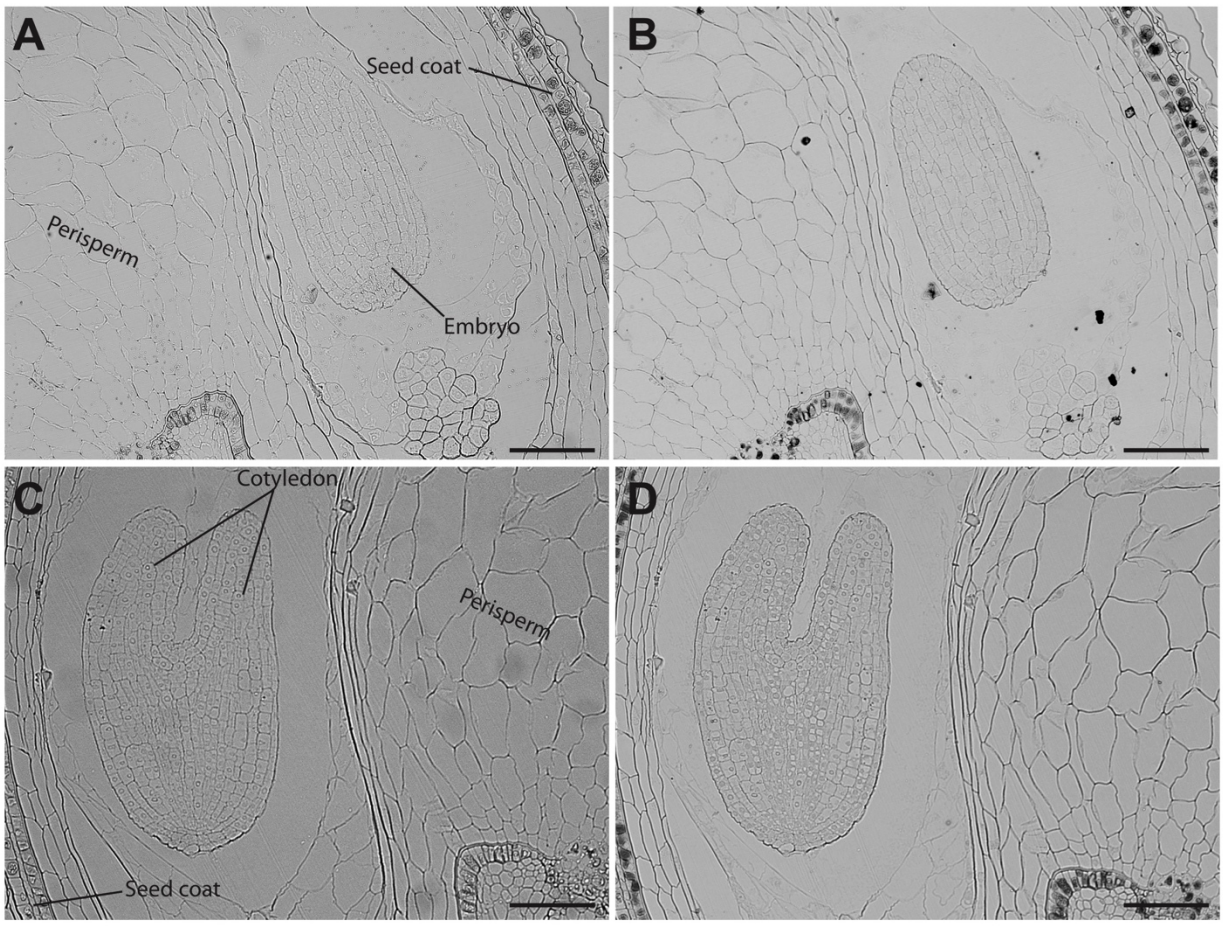

Figure 4. Iron distribution in *Chenopodium quinoa* seeds in early developmental stages. *Chenopodium quinoa* seeds 3 and 7 days post anthesis were collected from fruits, embedded in Technovit resin, sectioned (3 μm) and then stained with Perls/DAB (B and D). Unstained sections were used as control (A and C). The scale bar represents 100 μm.

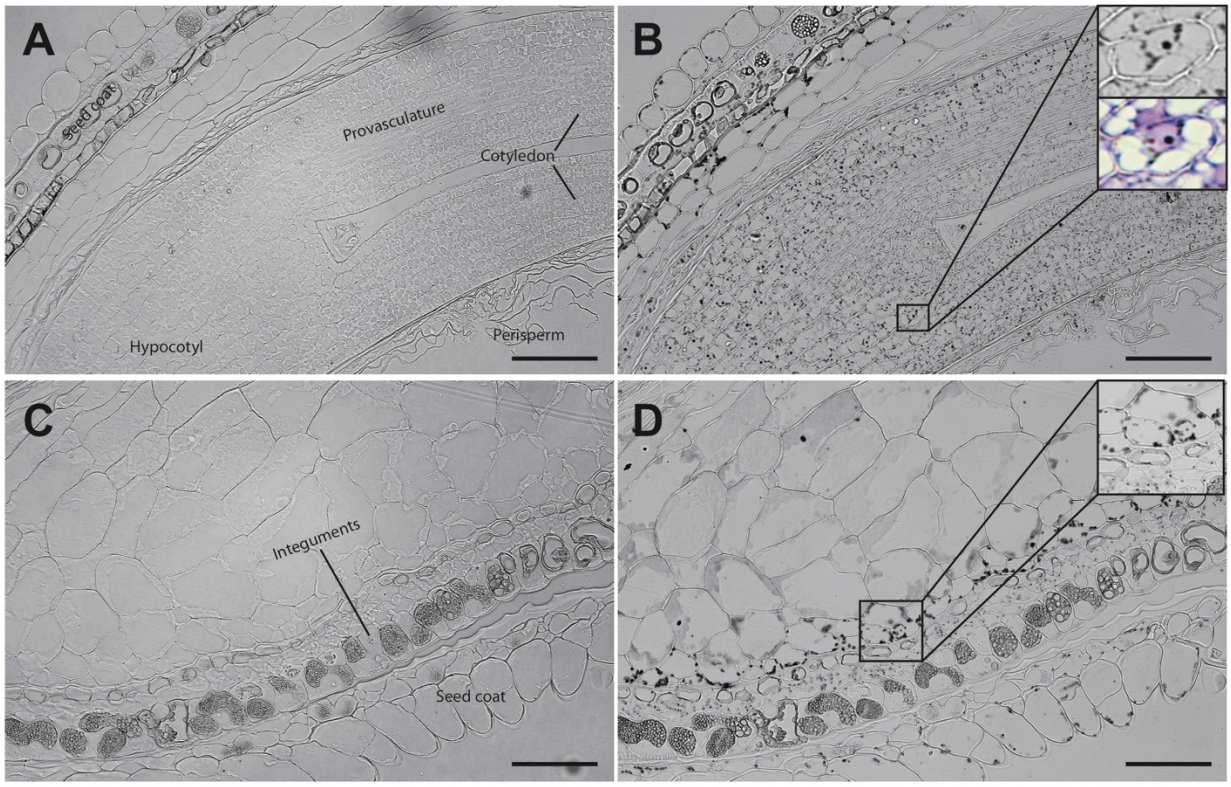

Figure 5. Iron distribution in *Chenopodium quinoa* seeds at cotyledon stage. *Chenopodium quinoa* seeds at the cotyledon stage (14 days post anthesis) dissected from fruits were embedded in Technovit resin, sectioned (3 μm) and then stained with Perls/DAB (B and D). In B the zoom shows iron accumulation into and around the nuclei. In B and D toluidine blue was used to show different cell structures. Unstained sections were used as control (A and C). The scale bar represents 100 μm.

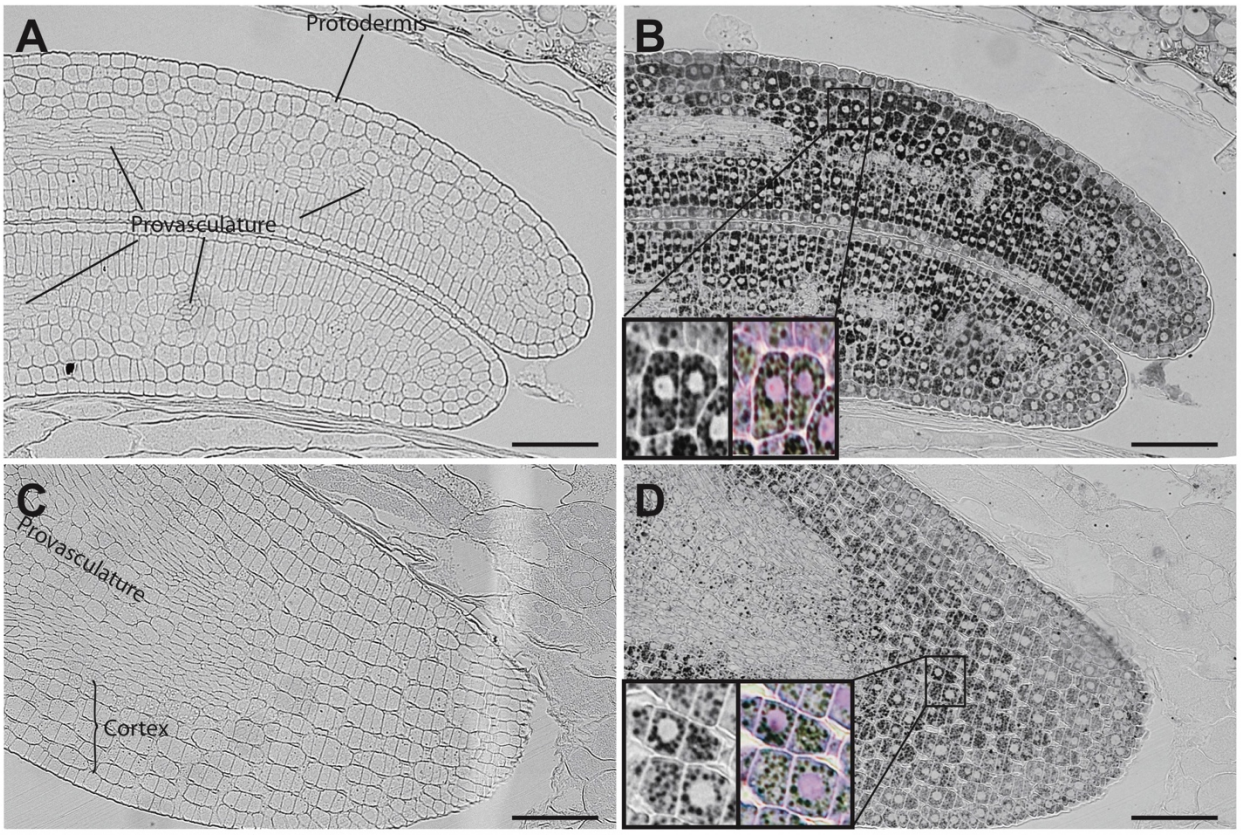

Figure 6. Iron distribution in *Chenopodium quinoa* seeds at mature embryo stage. *Chenopodium quinoa* seeds at the mature embryo stage, before seed desiccation stage (21 days post anthesis), were collected from fruits, embedded in Technovit resin and sectioned (3 µm). The sections were then stained with Perls/DAB (B and D). Cotyledons and hypocotyl are shown in A-B and C-D respectively. The zoom in B and D show iron accumulation in cell structures different from nuclei. Perls/DAB and Toluidine blue were used in order to reveal different cell structures. Unstained sections were used as control (A and C). The scale bar represents 100 µm.

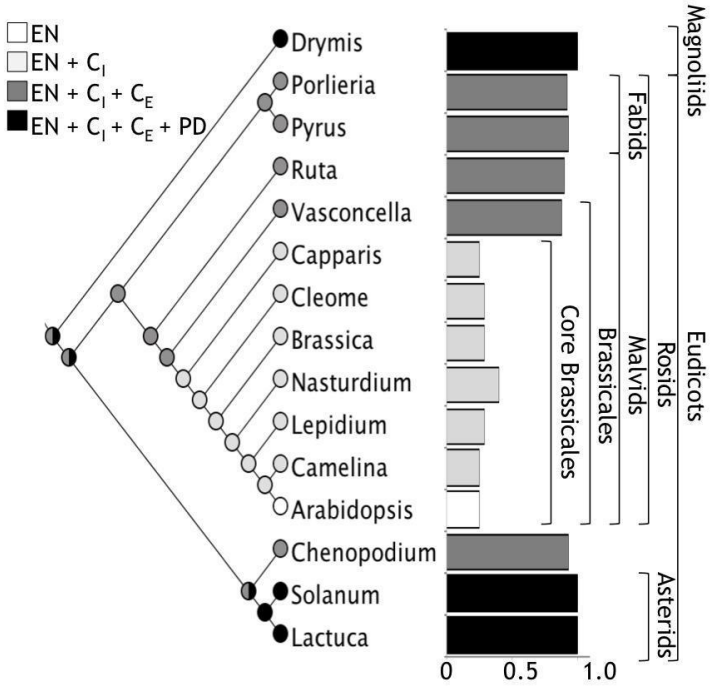

Figure 7. A global view of iron distribution in embryos. Phylogenetic tree showing all the species analyzed in this study. Colors of circles indicate type of cells that accumulate iron in the hypocotyl. White, only endodermis; light gray, endodermis + internal cortex (C_I); dark gray, endodermis + internal cortex + external cortex (C_E); black, endodermis + internal cortex + external cortex + protodermis (PD). Cortex cell are defined as the cell layers that are between the endodermis and the protodermis, we refer as internal cortex the cell layers than are near to the endodermis. Ratio of number of cells where iron is accumulated versus total number of cell layers from the endodermis to the protodermis for embryos from different orders are indicated in bars. Colors of bars correspond to the same code described above.

Supplemental table 1. List of seed embryos used in this study indicating the Order, Family and the name for each Species.

Order	Family	Species	Endodermis[a]	Cortex[a]	Protodermis[a]
Brassicales	Brassicaceae	*Arabidopsis thaliana*	X		
	Brassicaceae	*Camelina sativa*	X	X	
	Brassicaceae	*Nasturdium officinale*	X	X	
	Brassicaceae	*Lepidium sativum*	X	X	
	Brassicaceae	*Brassica napus*	X	X	
	Cleomaceae	*Cleome hassleriana*	X	X	
	Capparaceae	*Capparis spinosa*	X	X	
	Caricaceae	*Vasconcellea pubescens*	X	X	
Sapindales	Rutaceae	*Ruta graveolens*	X	X	
Rosales	Rosaceae	*Pyrus communis*	X	X	
Zygophyllales	Porlieria	*Porlieria chilensis*	X	X	
Solanales	Solanaceae	*Capsicum annuum*	X	X	
	Solanaceae	*Solanum lycopersicum*	X	X	X
Asterales	Asteraceae	*Lactuca sativa*	X	X	X
Caryophyllales	Polygonaceae	*Rumex acetosa*	X	X	X
	Polygonaceae	*Rheum rhaponticum*	X	X	
	Polygonaceae	*Fagopyrum esculentum*	X	X	
	Phytolaccaceae	*Phytolacca dioica*	X	X	
	Amaranthaceae	*Chenopodium quinoa*	X	X	
	Amaranthaceae	*Spinacia oleracea*	X	X	
	Amaranthaceae	*Beta vulgaris*	X	X	
Canellales	Winteraceae	*Drimys winteri*	X	X	X

[a]Letter X indicates detectable iron by Perls/DAB staining for each cell layer.

Table S1. List of seed embryos used in this study incidating the Orther, Family and the name of each Species.

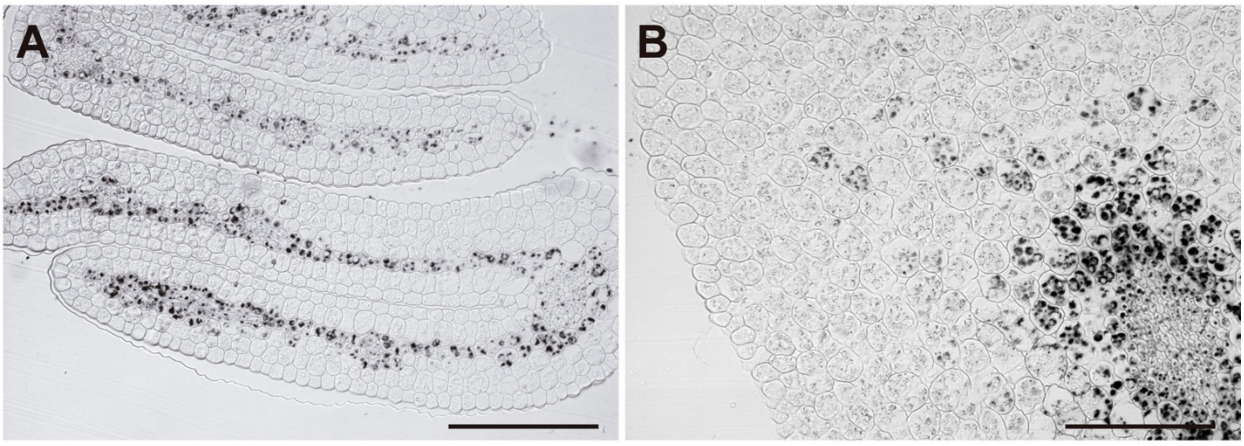

Figure S1. Iron distribution in dry seed embryo from *Capparis spinosa.* Embryos were disected from dry seeds and thin sections were obtained and stained with Perls/DAB in order to reveal iron accumulation. Cotyledon longitudinal sections and hypocotyl transversal section are shown (A and B). Bars in panels represents 100 μm

Capítulo 3 : Acumulación de hierro en semillas de *Chenopodium quinoa.*

La suficiencia de micronutrientes es un requisito fundamental para el bienestar de los humanos. En la dieta humana los micronutrientes son obtenidos principalmente desde las plantas, en particular por el consumo de semillas (Pongrac *et al.,* 2020). Sin embargo, muchos de los micronutrientes (manganeso, hierro, cobre y zinc) en granos suelen estar asociados a fitato, una sal rica en fósforo que no puede ser digerida por mamíferos. Dentro de estos minerales, el hierro es uno de los más importantes, tanto desde el punto de vista agronómico como de salud humana (Majeed *et al.,* 2020). El déficit de este nutriente produce un fenotipo de clorosis internerval en hojas jóvenes de la planta, afectando la reproducción y productividad de los cultivos (Zhu *et al.,* 2016). Además, la Organización Mundial de la Salud (OMS) ha estimado que alrededor de un 30% de la población padece de anemia por déficit de hierro, por lo que aumentar el contenido de hierro en las semillas en forma biodisponible ha sido sugerido como una buena alternativa para combatir la anemia por déficit de hierro (Murgia *et al.,* 2012).

Chenopodium quinoa Willd o quinoa es un pseudocereal originario del altiplano cuyo cultivo se está expandiendo globalmente. Durante las últimas décadas el número de países cultivadores quinoa ha aumentado en un 10%, principalmente debido a que quinoa presenta resistencia a distintos tipos de estrés abiótico y su semilla posee un alto valor nutricional (Bazile *et al.,* 2016). Comparada con otros cereales, las semillas de quinoa son libres de gluten y presentan un mejor balance de proteínas, lípidos, carbohidratos y aminoácidos esenciales, además de ser muy ricas en nutrientes (Nowak *et al.,* 2016; Woolf, *et al*., 2011). Quinoa pertenece a la familia de las *Amaranthaceae*, es alotetraploide (2n = 4x = 36), y su genoma fue recientemente secuenciado, abriendo las

puertas al desarrollo de estrategias de biología molecular en esta planta (Zou *et al.,* 2017).

La semilla de quinoa contiene entre 3 y 5 veces más hierro que la semilla de Arabidopsis (Kim *et* al., *2006;* Valencia *et al.,* 1999). Además, recientemente fuimos capaces de describir que quinoa presenta un patrón de acumulación y distribución de hierro distinto al observado en Brassicaceae (Ibeas *et al.,* 2017; Ibeas *et al.,* 2019). Sin embargo, aún se desconoce dónde se almacena el hierro en esta planta ni los ligandos que se utilizan tanto para el almacenamiento como para la movilización de este nutriente.

Un estudio de ultraestructura realizado en semillas de quinoa reveló que las semillas de quinoa poseen una gran cantidad de gránulos de almidón acumulados principalmente en el perisperma, mientras que el embrión está enriquecido en vacuolas con cuerpos lipídicos y cuerpos proteicos (con estructura de tipo globoide), además de poseer una gran cantidad de proplastidios con depósitos de ferritinas en su interior. Análisis de EDX (*Energy Dispersive X-Ray Spectroscopy*) permitieron determinar que las estructuras tipo globoide acumulan potasio, magnesio y fósforo, pero no hierro (Prego *et al.,* 1998). Las ferritinas son una clase universal de proteínas multiméricas de almacenamiento de hierro, teniendo una capacidad de entre 2.000 a 4.000 átomos de hierro en su cavidad central (Briat *et al.,* 2010; Ravet *et al.,* 2009). En Arabidopsis ha sido establecido que las ferritinas actuarían como un mecanismo de control de la concentración de hierro libre en condiciones de estrés, para así evitar la producción de especies reactivas de oxígeno. Arabidopsis posee cuatro genes que codifican para ferritinas, de los cuales solo uno se expresa en semilla (*FER2*). Plantas mutantes para *FER2* no presentan alteraciones en el contenido ni distribución de hierro, ni tampoco se ve afectada su capacidad de

germinación ni desarrollo post-germinativo (Ravet *et al.,* 2009). En lo que respecta a quinoa, aún no se ha establecido el papel que poseen las ferritinas en las semillas, sin embargo, el hecho de que las vacuolas de quinoa no acumulen grandes cantidades de hierro, acompañado de la alta presencia de depósitos de ferritinas en el embrión, abre nuevas preguntas respecto a cuáles son los mecanismos empleados por quinoa para la acumulación y distribución de hierro en las semillas de esta planta.

MATERIALES Y MÉTODOS

Inmunodetección de ferritinas mediante Western Blot.

Proteínas totales de embriones aislados de Quinoa o de semillas enteras de *Arabidopsis thaliana* fueron extraídas de la siguiente manera. 20 µg del tejido correspondiente fueron congelados en nitrógeno líquido y homogenizados en un Fast-Prep-24 Instrument (MP Biomedicals) siguiendo las recomendaciones del fabricante. Los tejidos homogenizados fueron resuspendidos en 500 µL de buffer Urea/Thiourea (7 M Urea, 2 M Thiourea, 4% CHAMPS, 1% DTT en 30 mM Tris-HCl, pH 8,5) y fueron agitadas durante 30 minutos a 4 ºC. Luego se centrifugaron a 5000 g a 4 ºC durante 30 minutos. Luego de recuperar el sobrenadante, el contenido total de proteínas fue cuantificado utilizando el método de Bradford. Le electroforesis en geles de poliacrilamida y transferencia a la membrana fueron realizados según fue descrito en Tissot *et al.,* 2019. La inmunodetección fue revelada utilizando el kit Supersignal West Pico Plus (Thermo Scientific) según las indicaciones del fabricante.

Inmunodetección de ferritinas en cortes histológicos de semillas.

Para realizar la inmunodetección, embriones aislados fueron fijados en paraformaldehído 4% en PBS 0,01 M, pH 7,4 y una gota de Tween-80. Las muestras fueron incubadas a 4 ºC con agitación constante durante toda la noche. Luego se realizaron dos lavados con glicina en buffer PBS. La deshidratación fue realizada utilizando baños consecutivos con etanol 50%, etanol 70%, una solución etanol-butanol 1:1, butanol 100% y finalmente butanol-parafina en un *Histos 5 microwave tissue processor* (Rankin Biomedical). Cortes histológicos de 8 µm fueron generados. La parafina fue eliminada de las muestras utilizando la solución *SafeSolv* y las muestras fueron rehidratadas con baños consecutivos de etanol 100%, etanol 70%, etanol 50% y buffer PBS. Posteriormente las muestras fueron tratadas con Tripsina 0,1% durante 8 minutos y luego fueron bloqueadas con una solución al 6% de FBS (*Fetal Bovine Serum*). Las muestras fueron incubadas durante toda la noche a 4 ºC con el anticuerpo primario purificado anti-FERRITINs (rabbit) 8 µg/mL in FBS. Las muestras fueron lavadas con PBS y finalmente fueron incubadas con el anticuerpo secundario Alexa488 anti-rabbit 1/500 (Molecular Probes) en 3% FBS. Finalmente se montaron las muestras en Mowiol y fueron analizadas en un microscopio de epifluorescencia.

RESULTADOS

Análisis de inmunodetección de Ferritinas en extractos de proteínas totales de Quinoa y Arabidopsis mostraron la presencia de Ferritinas (peso molecular teórico de aproximadamente 25 KDa) utilizando un suero policlonal anti-Ferritinas de Arabidopsis (Ravet *et al.,* 2009). Extractos de proteínas obtenidos desde semillas silvestres mutantes para los genes *fer2* y *fer134* de *Arabidopsis thaliana,* fueron utilizados como control del experimento. En primera instancia se realizó el experimento utilizando extractos que

contenían 10 y 5 ug de proteínas totales de embriones aislados de quinoa con lo cual solo fue posible visualizar una banda de gran tamaño que posiblemente corresponde a ferritinas (Figura 1A). Para optimizar la resolución de bandas de este experimento, se repitió utilizando menos cantidad de proteínas. La Figura 1B muestra la detección de una única banda de 25 KDa aproximadamente, correspondiente a Ferritinas en 1 ug de extracto total de proteínas de embriones aislados de quinoa. Esto nos permite confirmar la presencia de Ferritinas en embriones de quinoa y sugiere además que acumulan una gran cantidad de ferritinas comparado con Arabidopsis. En el caso de las muestras de Arabidopsis, se utilizaron 10 ug de extracto total de proteínas para ambos experimentos.

Finalmente, se realizó una inmuno-detección en cortes histológicos de semilla de quinoa para determinar si la marca de hierro detectada mediante la tinción Perls/DAB estaba asociada de algún modo a la presencia de complejos hierro-Ferritina. Estos complejos han sido detectados exitosamente utilizando hojas de Arabidopsis tratadas con exceso de hierro (Roschzttardtz *et al,* 2013). Cortes histológicos de hipocotilo de quinoa muestra detección de ferritinas en un patrón punteado en distintos tipos celulares, incluyendo la endodermis, el córtex y la provasculatura (Figura 2A y B). Cortes histológicos de semillas de *fer2-1* fueron utilizados como control negativo mientras que cortes de mutantes *fer134* fueron utilizados como control positivo (Figura 2 C-F). Este patrón de distribución de Ferritinas es muy similar al patrón de distribución de hierro observado con la tinción Perls/DAB en embriones de quinoa, sugiriendo que en estas semillas es posible que las reservas de hierro se acumulen en complejos hierro-Ferritina.

Finalmente, para determinar dónde se localizan las principales reservas de hierro en la semilla de quinoa evaluamos la concentración de hierro total acumulada en embriones

aislados y en semillas completas de quinoa. Ambos tejidos fueron aislados y una digestión ácida fue realizada, para posteriormente ser evaluadas mediante MP-AES (Microwave Plasma-Atomic Emission Spectrometry; Figura 3). La concentración de hierro obtenida para semilla seca fue de 70,069 ug de hierro por gramo de semillas, mientras que embriones aislados se obtuvo 228,3 ug de hierro por gramo de embriones aislados. Considerando que el embrión ocupa alrededor del 30% del volumen total de la semilla de quinoa, esta información sugiere que la mayor cantidad de reservas de quinoa se localizan en la porción del embrión de la semilla.

DISCUSIÓN

La deficiencia de hierro se ha presentado como uno de los principales desórdenes alimenticios para los humanos afectando a más de 2 millones de personas en el mundo, siendo las mujeres en edad fértil y los niños menores de dos años el grupo más vulnerable al déficit de este nutriente (Murgia *et al.,* 2012). Dado que las semillas son una de las principales fuentes de alimento para los animales y humanos, encontrar la forma de aumentar el valor nutricional de las semillas se ha vuelto esencial durante las últimas décadas. Es por esto que comprender los mecanismos moleculares involucrados en la distribución y almacenamiento de hierro en semillas es fundamental para el desarrollo de nuevas aproximaciones biotecnológicas que permitan mejorar el contenido de hierro en semillas.

Utilizando distintas metodologías de detección de hierro en tejidos vegetales, fue posible observar que en Arabidopsis el hierro se acumula en las vacuolas de las células de la endodermis del embrión (Kim *et al.,* 2006; Roschzttardtz *et al.,* 2009). Si bien, este patrón

de distribución es bastante conservado en otros miembros de la familia de las Brassicaceaes, no está presente en todas las especies, lo que sugiere que los embriones pueden presentar diversas estrategias para almacenar el hierro (Ibeas *et al.,* 2019).

Las semillas de quinoa poseen un alto valor nutricional y han sido utilizadas exitosamente como un nuevo alimento funcional. Estas semillas poseen entre 3 y 5 veces más hierro que las semillas de Arabidopsis, y pueden cubrir las necesidades alimentarias de hierro en niños y adultos (Konishi *et al.,* 2004; National Academy Press, 2001). Utilizando la tinción Perls/DAB fuimos capaces de evaluar la distribución de hierro durante distintos estadios de desarrollo de la semilla de quinoa. En este estudio, observamos que el patrón de acumulación de hierro durante el desarrollo de la semilla en quinoa es distinto, sobre todo en los primeros estados analizados, a lo que observamos previamente en *B. napus,* una especie cercana filogenéticamente hablando a Arabidopsis, donde el hierro se acumulaba en el núcleo en el endosperma y en distintos tipos celulares del embrión en estado torpedo, mientras que en quinoa observamos que ningún tipo celular de la semilla acumula hierro en los primeros estados de desarrollo. Lo que apoya la idea de la existencia de diversos mecanismos de acumulación y movilización de hierro en semillas (Ibeas *et al.,* 2017; Ibeas *et al.,* 2019).

Determinar dónde se están acumulando las reservas de hierro es esencial para el desarrollo de nuevas estrategias que permitan la obtención de alimentos funcionales. Cómo se ha mencionado anteriormente, en el caso de la planta modelo *Arabidopsis thaliana*, el hierro se acumula principalmente en vacuolas mientras, que las ferritinas poseen una función menor en este proceso (Ravet *et al.,* 2009). Sin embargo, esto no es

algo conservado en todas las especies, ya que hay algunas legumbres que acumulan hasta un 70% de la porción total de hierro en ferritinas (Moore *et al.,* 2018).

Las ferritinas son una clase universal de proteínas de almacenamiento de hierro, forman complejos supramoleculares que pueden acumular más de 4000 átomos de hierro lo que les permite controlar la cantidad de hierro libre en la célula, evitando la formación de especies reactivas de oxígeno en la célula (Briat *et al.,* 2010). Previamente ha sido descrito que los principales componentes de almacenamiento del embrión de quinoa son cuerpos lipídicos, cuerpos proteícos con estructuras de tipo globoides y proplastidios con altos depósitos de fitoferritinas (Prego *et al.,* 1998). En este mismo estudio, un análisis de composición elemental de la semilla de quinoa mostró que las vacuolas del embrión de quinoa no acumulan grandes cantidades de hierro, lo que abre la pregunta ¿dónde se están acumulando las reservas de hierro en la semilla de quinoa? Y si es posible que el alto contenido de ferritinas presente en la semilla esté asociada a la acumulación de hierro.

Si bien las ferritinas de plantas poseen un origen Eucarionte y su secuencia de aminoácidos de bien conservada con las ferritinas de animales (Ragland *et al.,* 1999), poseen características únicas al ser comparadas con ferritinas de orígenes distintos. Por ejemplo, son sintetizadas como precursores con una extensión de aminoácidos en el N-Terminal que solo ha sido observada en plantas. Esta fracción se divide en dos partes, el péptido de extensión y un péptido de tránsito responsable de la localización subelular de las ferritinas en plantas. Cabe mencionar que en plantas las ferritinas nunca se localizan en el citoplasma y en efecto, suelen localizarse en plástidos no verdes. En

efecto, es posible localizar ferritinas en cloroplastos solo en respuesta a estrés (Briat *et al.,* 2010).

En el caso de Arabidopsis, las ferritinas son codificadas por una pequeña familia de 4 miembros (*FERRITIN1-4; FER1-4*) y algunos estudios han sido realizados para comprender su perfil de expresión y cinética durante el ciclo de vida de la planta (Petit *et al.,* 2001). Por un lado, el transcrito de *FER1* y *FER3* se acumula con abundancia en las hojas de la roceta y en estados tardíos de desarrollo de la planta; por otro lado, la expresión de *FER2* se encuentra restringida principalmente a la semila mientras que la expresión de *FER4* se restringe a botones florales y flores después de la polinización (Petit *et al.,* 2001). A nivel proteíco, utilizando un suero policlonal que detecta ferritinas, mediante ensayos de western blot con extractos crudos de proteínas fue posible identificar que *FER1* se acumula principalmente en hojas como una subunidad de 28 kDa, mientras que la *FER3 y FER4* existen en hoja como una subunidad procesada de 26,5 kDa aproximadamente. Finalmente, la *FER2* es la única ferritina presente en semillas, como una subunidad de 26,5 kDa aproximadamente (Ravet *et al.,* 2009).

Utilizando la secuencia genómica de quinoa, identificamos 4 genes putativos que podrían codificar para ferritinas, AUR62022943, AUR62030516, AUR62012304 y AUR62030776 respectivamente (https://phytozome.jgi.doe.gov/pz/portal.html). Estudios para tratar de identificar la secuencia aminoacídica muestra que AUR62022943 y AUR62030776 codifican para una secuencia de proteínas de alrededor de 22 kDa, mientras que AUR62030516 y AUR62012304 codifican para una proteína putativa de alrededor de 28 kDa (https://web.expasy.org/compute_pi/). Análisis de alineamientos múltiples de secuencias aminoacídicas mostraron que a nivel proteíco, la secuencia aminoacídica

codificada por estos genes posee entre un 72 y 80 de identidad con *FER1,* 67 y 77% con *FER2,* 68 y 78% con *FER3,* y entre un 77 y 80% con *FER4*.

Debido a la alta identidad que poseen las proteínas de quinoa con las de Arabidopsis, evaluamos mediante Western Blot la acumulación de ferritinas en extractos totales de semillas de quinoa. Resultados preliminares para este experimento mostraron una única banda con un peso inferior a los 25 kDa, lo que sugiere que puede ser una proteína codificada por AUR62022943 y/o AUR62030776. Sin embargo, es necesario hacer un seguimiento del perfil de acumulación y expresión del mRNA en distintos tejidos de quinoa para poder saber si la expresión de estos genes es ubicua o si presentan un comportamiento similar al tejido/estadio específico observado por las ferritinas de Arabidopsis.

Además, de manera preliminar fuimos capaces de evaluar la distribución de ferritinas en los distintos tipos celulares del embrión de quinoa (Figura 2). En este experimento fuimos capaces de observar un patrón punteado en distintos tipos celulares del embrión de quinoa, incluyendo la endodermis y las células del córtex, muy similar al patrón de distribución de hierro observado en estas semillas. Esta correlación en la localización de las reservas de hierro y los complejos de ferritina, sumado a que Prego *et al.,* describió que las vacuolas del embrión de quinoa no acumulan hierro, nos permite suponer que posiblemente las ferritinas de quinoa puedan estar acumulando las reservas de este metal en el embrión. Sin embargo, es necesario hacer más estudios para poder confirmar esta hipótesis.

CONCLUSIONES

- Se obtuvo el primer estudio filogenético de distribución de hierro en semillas.
- El patrón de distribución de hierro observado en Arabidopsis corresponde a un carácter apomórfico.
- Durante la maduracion del embrión de *B. napus*, el hierro se acumula en distintos compartimentos subcellulares antes de entrar a la vacuola de la endodermis.
- Nuestros datos sugieren que existe una correlación entre el hierro acumulado en el embrión de quinoa y la presencia de ferritinas en todos los tipos celulares del embrión.
- Las principales reservas de hierro en una semilla de C. quinoa se encuentran acumuladas en el embrión.

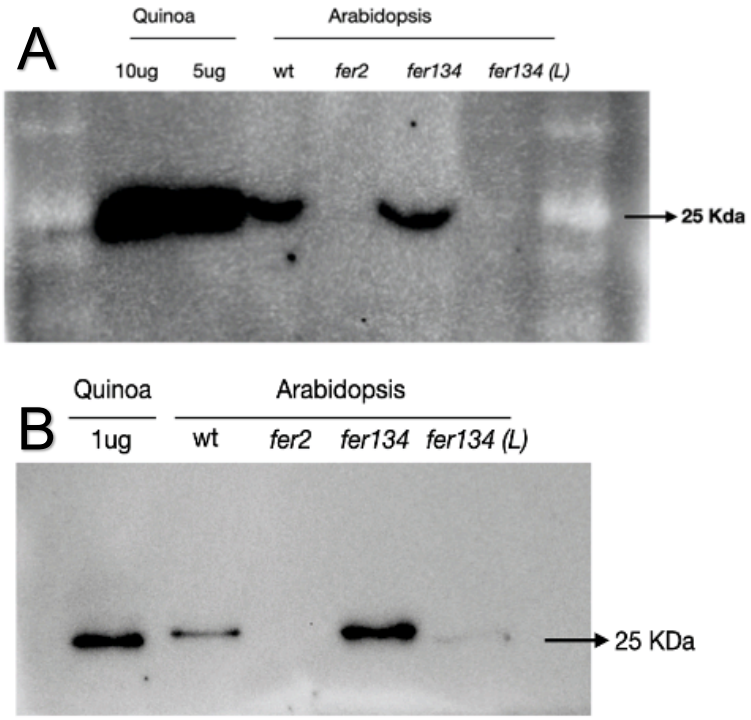

Figura 1. Inmunodetección de Ferritinas mediante Western Blot. La acumulación de Ferritinas en semillas de quinoa fue evaluada. Extractos de proteínas totales (10 y 5 ug en A, 1 ug en B) de quinoa fueron separados por SDS-PAGE y transferidos a una membrana. 10 ug de extractos de proteínas totales de semillas Arabidopsis col-0, *fer2, fer134,* y hojas de *fer134* regadas con 2 mM de una solución de Fe-EDDHA fueron utilizadas como control.

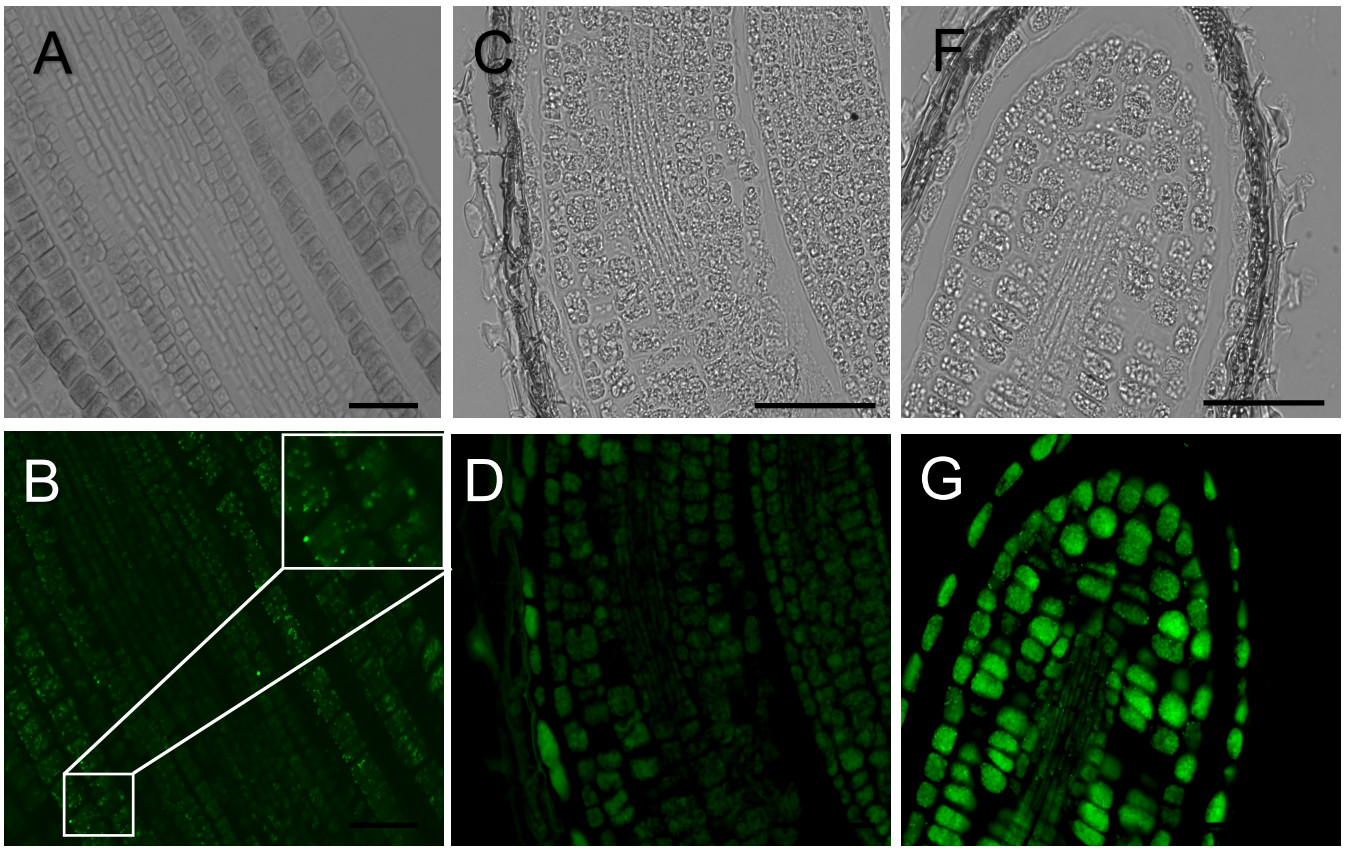

Figura 2. Inmunodetección de Ferritinas en cortes histológicos de quinoa. La distribución de ferritinas en cortes histológicos de semillas de quinoa fue evaluada. Cortes histológicos de 8 µm fueron analizados. A, C y F muestran el campo claro; B, D y G muestran la distribución de ferritinas observadas para embriones de quinoa, *fer2-1* y *fer134* respectivamente. *fer2-1* fue utilizado como control negativo del experimento. Un zoom fue realizado en el panel B para observar mejor la marca de ferritina observada en células del cortex del embrión. La barra de tamaño representa 100 µm.

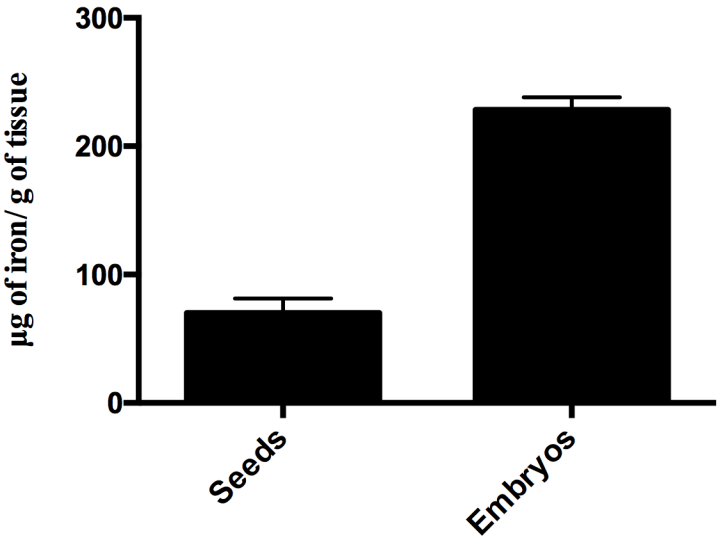

Figura 3. Concentraión de hierro en semillas y embriones de *Chenopodium quinoa*. Contenido de hierro en semillas de quinoa determinado por MP-AES. Los gráficos representan el promedio de 4 réplicas biológicas para cada tejido.

REFERENCIAS

- Abugoch L. (2009) Advances in food and nutrition research. Volume 58, Elsevier Inc.
- Aloisi, Iris, Luigi Parrotta, Karina B. Ruiz, Claudia Landi, Luca Bini, Giampiero Cai, Stefania Biondi, and Stefano Del Duca. 2016. “New Insight into Quinoa Seed Quality under Salinity: Changes in Proteomic and Amino Acid Profiles, Phenolic Content, and Antioxidant Activity of Protein Extracts.” Frontiers in Plant Science 7 (May): 1–21. doi:10.3389/fpls.2016.00656.
- APG IV (2016) An update of the Angiosperm Phylogeny Group classification for the orders and families of flowering plants: APG IV. Botanical Journal of the Linnean Society, 181:1-20.
- Bashir, Khurram, Yasuhiro Ishimaru, Hugo Shimo, Seiji Nagasaka, Masaru Fujimoto, Hideki Takanashi, Nobuhiro Tsutsumi, Gynheung An, Hiromi Nakanishi, and Naoko K. Nishizawa. 2011. “The Rice Mitochondrial Iron Transporter Is Essential for Plant Growth.” Nature Communications 2: 322. doi:10.1038/ncomms1326.
- Bazile D, Jacobsen SE, Verniau A . The global expansion of quinoa: trends and limits. *Front Plant Sci* 2016; **7**:622.
- Beilstein M., Nagalingum N., Clements M., Manchester S., Mathews S. (2010) Dated molecular phylogenies indicate a Miocene origin for *Arabidopsis thaliana*. Proceedings of the National Academy of Sciences, 107:18724-18728.
- Briat, Jean François, Céline Duc, Karl Ravet, and Frédéric Gaymard. 2010. “Ferritins and Iron Storage in Plants.” Biochimica et Biophysica Acta - General Subjects 1800 (8). Elsevier B.V.: 806–14. doi:10.1016/j.bbagen.2009.12.003.

- Briat, Jean Francois, Karl Ravet, Nicolas Arnaud, Céline Duc, Jossia Boucherez, Brigitte Touraine, Francoise Cellier, and Frederic Gaymard. 2010. “New Insights into Ferritin Synthesis and Function Highlight a Link between Iron Homeostasis and Oxidative Stress in Plants.” Annals of Botany 105 (5): 811–22. doi:10.1093/aob/mcp128.
- Cavell A., Lydiate D., Parkin I., Dean C., Trick M. (1998) Collinearity between a 30-centimorgan segment of Arabidopsis thaliana chromosome 4 and duplicated regions within the Brassica napus genome. *Genome*, **41**, 62–69.
- Chen BY., Zhao BC., Li MF., Liu QY, and Sun RC. (2017) Bioresource Technology Fractionation of Rapeseed Straw by Hydrothermal/Dilute Acid Pretreatment Combined with Alkali Post-Treatment for Improving Its Enzymatic Hydrolysis. Bioresource Technology (225)127–33.
- Cotte M., Pouyet E., Salomé M., Rivard C., De Nolf W., Castillo-Michel H., Fabris T., Monico L., Janssens K., Wang T., Sciau P., Verger L., Cormier L., Dargaud O., Brun E., Bugnazet D., Fayard B., Hesse B., Pradas del Real A., Veronesi G., Langlois J., Balcar N., Vandenberghe Y., Solé V., Kieffer J., Barrett R., Cohen C., Cornu C., Baker R., Gagliardini E., Papillon E., Susini J. (2017) The ID21 X-ray and infrared microscopy beamline at the ESRF: status and recent applications to artistic materials. Journal of Analytical Atomic Spectrometry, 32:477–493.
- Curie, Catherine, and Jean-François Briat. 2003. “Iron transport and signaling in plants.” Annual Review of Plant Biology 54 (1): 183–206. doi:10.1146/annurev.arplant.54.031902.135018.

- Curie, Catherine, Gaëlle Cassin, Daniel Couch, Fanchon Divol, Kyoko Higuchi, Marie Le Jean, Julie Misson, Adam Schikora, Pierre Czernic, and Stéphane Mari. 2009. “Metal Movement within the Plant: Contribution of Nicotianamine and Yellow Stripe 1-like Transporters.” Annals of Botany 103 (1): 1–11. doi:10.1093/aob/mcn207.
- Cvitanich C., Przybyłowicz W., Urbanski D., Jurkiewicz A., Mesjasz-Przybyłowicz J., Blair M., Stougaard, J. (2010). Iron and ferritin accumulate in separate cellular locations in Phaseolus seeds. BMC Plant Biology, 10:26.
- De Brier N., Gomand S., Donner E., Paterson D., Smolders E., Delcour J., Lombi E. (2016) Element distribution and iron speciation in mature wheat grains (Triticum aestivum L.) using synchrotron X-ray fluorescence microscopy mapping and X-ray absorption near-edge structure (XANES) imaging. Plant Cell Environ, 39:1835-47.
- DeFries R., Fanzo J., Remans R., Palm C., Wood S. Anderman, T. L. (2015). Global nutrition. Metrics for land-scarce agriculture. Science, 349:238–240.
- Divol, F., D. Couch, G. Conejero, H. Roschzttardtz, S. Mari, and C. Curie. 2013. “The Arabidopsis YELLOW STRIPE LIKE4 and 6 Transporters Control Iron Release from the Chloroplast.” The Plant Cell 25 (3): 1040–55. doi:10.1105/tpc.112.107672.
- Eroglu S., Giehl RFH., Meier B., Takahashi M., Terada Y., Ignatyev K., Andresen E., Küpper H., Peiter E., von Wirén N. (2017) Metal tolerance protein 8 mediates manganese homeostasis and iron reallocation during seed development and germination. Plant Physiology, 174:1633-1647.
- Fan M., Zhao F., Fairweather-Tait S., Poulton P., Dunham S., McGrath S. (2008). Evidence of decreasing mineral density in wheat grain over the last 160 years. Journal of Trace Elements in Medicine and Biology, 22, 315-324.

- Flis P., Ouerdane L., Grillet L., Curie C., Mari S., Lobinski R. (2016) Inventory of metal complexes circulating in plant fluids: a reliable method based on HPLC coupled with dual elemental and high-resolution molecular mass spectrometric detection. New Phytologist, 211:1129-41.
- Grillet, L., Lan, P., Li, W. *et al.* IRON MAN is a ubiquitous family of peptides that control iron transport in plants. *Nature Plants* **4,** 953–963 (2018). https://doi.org/10.1038/s41477-018-0266-y
- Grillet, Louis, Stéphane Mari, and Wolfgang Schmidt. 2014. “Iron in Seeds – Loading Pathways and Subcellular Localization.” Frontiers in Plant Science 4 (January): 535. doi:10.3389/fpls.2013.00535.
- Grillet L., Ouerdane L., Flis P., Hoang M., Isaure M., Lobinski R., Curie C., Mari S. (2014) Ascorbate efflux as a new strategy for iron reduction and transport in plants. J. Biol. Chem. 289:2515-25.
- Guerinot M., Yi Y. (1994) Iron: nutritious, noxious, and not readily available. Plant Physiology, 104:815–820.
- Guo X,, Hao G., Zhang L., Mao K., Wang X., Zhang D., Ma T., Hu Q., Ihsan A., Al-Shehbaz Koch M. (2017) Plastome phylogeny and early diversification of Brassicaceae. BMC Genomics, 18:176.
- Hall J., Iltis H., Sytsma K. (2004) Molecular phylogenetics of core brassicales, placement of orphan genera rmblingia, forchhammeria, tirania, and character evolution. Systematic Botany, 29: 654–669.

- Ibeas M., Grant-Grant S., Navarro N., Perez M., Roschzttardtz H. (2017) Dynamic subcellular localization of iron during embryo development in Brassicaceae seeds. Front Plant Sci, 8:2186.
- Ibeas MA, Grant-Grant S, Coronas MF, Vargas-Pérez JI, Navarro N, Abreu I, Castillo-Michel H, Avalos-Cembrano N, Paez Valencia J, Perez F, González-Guerrero M and Roschzttardtz H (2019) The Diverse Iron Distribution in Eudicotyledoneae Seeds: From Arabidopsis to Quinoa. *Front. Plant Sci.* 9:1985. doi: 10.3389/fpls.2018.01985
- Hilo A., Shahinnia F., Druege U., Franken P., Melzer M., Rutten T., von Wirén N., Hajirezaei M. (2017) A specific role of iron in promoting meristematic cell division during adventitious root formation, Journal of Experimental Botany, erx248, https://doi.org/10.1093/jxb/erx248
- Iwai T., Takahashi M., Oda K., Terada Y., Yoshida K. (2012) Dynamic changes in the distribution of minerals in relation to phytic acid accumulation during rice seed development. Plant Physiology, 160:2007-2014.
- Jarvis, David E., Yung Shwen Ho, Damien J. Lightfoot, Sandra M. Schmöckel, Bo Li, Theo J. A. Borm, Hajime Ohyanagi, et al. 2016. “The Genome of Chenopodium Quinoa.” Nature 542 (7641): 307–12. doi:10.1038/nature21370.
- Jeong, J., C. Cohu, L. Kerkeb, M. Pilon, E. L. Connolly, and M. L. Guerinot. 2008. “Chloroplast Fe(III) Chelate Reductase Activity Is Essential for Seedling Viability under Iron Limiting Conditions.” Proceedings of the National Academy of Sciences 105 (30): 10619–24. doi:10.1073/pnas.0708367105.
- Johnson A., Kyriacou B., Callahan D., Carruthers L., Stangoulis J., Lombi E., et al. (2011) Constitutive Overexpression of the *OsNAS* Gene Family Reveals Single-Gene

Strategies for Effective Iron- and Zinc-Biofortification of Rice Endosperm. PLoS ONE6(9): e24476.

- Kim, S. A., T. Punshon, A. Lanzirotti, L. Li, J. M. Alonso, J. R. Ecker, J. Kaplan, and M. L. Guerinot. 2006. “Localization of Iron in Arabidopsis Seed Requires the Vacuolar Membrane Transporter VIT1.” Science 314 (5803): 1295–98. doi:10.1126/science.1132563.
- Kobayashi, Takanori, and Naoko K. Nishizawa. 2012. “Iron Uptake, Translocation, and Regulation in Higher Plants.” Annual Review of Plant Biology 63 (1): 131–52. doi:10.1146/annurev-arplant-042811-105522.
- Konishi Y., Hirano S., Tsuboi H., Wada M. (2004) Distribution of minerals in quinoa (Chenopodium quinoa Willd.) seeds, Biosci Biotechnol Biochem, 68:231-234.
- Lanquar, Viviane, Françoise Lelièvre, Susanne Bolte, Cécile Hamès, Carine Alcon, Dieter Neumann, Gérard Vansuyt, et al. 2005. “Mobilization of Vacuolar Iron by AtNRAMP3 and AtNRAMP4 Is Essential for Seed Germination on Low Iron.” The EMBO Journal 24 (23): 4041–51. doi:10.1038/sj.emboj.7600864.
- Li, Wenfeng, and Ping Lan. 2017. “The Understanding of the Plant Iron Deficiency Responses in Strategy I Plants and the Role of Ethylene in This Process by Omic Approaches.” Frontiers in Plant Science 8 (January): 1–15. doi:10.3389/fpls.2017.00040.
- López-Fernández, María Paula, and Sara Maldonado. 2013. “Programmed Cell Death during Quinoa Perisperm Development.” Journal of Experimental Botany 64 (11): 3313–25. doi:10.1093/jxb/ert170.

- Lu L., Tian S., Liao H., Zhang J., Yang X., Labavitch J., Chen W. (2013) Analysis of metal element distributions in rice (Oryza sativa L.) seeds and relocation during germination based on X-Ray fluorescence imaging of Zn, Fe, K, Ca, and Mn. PLoS ONE, 8:e57360.
- Maddison W., Maddison D.. (2007) Mesquite: A modular system for evolutionary analysis, version 2.0.
- Majeed A, Minhas WA, Mehboob N, Farooq S, Hussain M, et al. (2020)Correction: Iron application improves yield, economic returns and grain-Fe concentration of mungbean. PLOS ONE 15(4): e0232150.
- Marschner H. Mineral nutrition of higher plants. 2. ed. Orlando: Academic Press, 2005. 889 p.
- Mary V., Schnell M., Gillet C., Socha A., Giraudat J., Agorio A., Merlot S., Clairet C., Kim S., Punshon T., Guerinot M., Thomine S. (2015) Bypassing iron storage in endodermal vacuoles rescues the iron mobilization defect in the natural resistance associated-macrophage protein3 natural resistance associated-macrophage protein4 double mutant. Plant Physiology, 169: 748–759.
- Moore, K. L., Rodríguez-Ramiro, I., Jones, E. R., Jones, E. J., Rodríguez-Celma, J., Halsey, K., et al. (2018). The stage of seed development influences iron bioavailability in pea (*Pisum sativum* L.). *Sci. Rep.* 8:6865. doi: 10.1038/s41598-018-25130-3
- Murgia I., Arosio P., Tarantino D., Soave C. (2012) Biofortification for combating 'hidden hunger' for iron. Trends Plant Sci, 17:47-55.

- National Academy Press. (2001) Dietary reference intakes for vitamin A, vitamin K, arsenic, boron, chromium, copper, iodine, iron, manganese, molybdenum, nickel, silicon, vanadium, and zinc. National Academy Press, USA.
- Nowak V, Du J, Charrondiere UR . Assessment of the nutritional composition of quinoa (*Chenopodium quinoa* Willd.). *Food Chem* 2016; **193**:47–54.
- Otegui MS., Capp R., Staehelin LA. (2002) Developing seeds of Arabidopsis store different minerals in two types of vacuoles and in the endoplasmic reticulum. Plant Cell,14:1311-27.
- Parkin, I., Sigrun M., Andrew G., Lewis L., Martin T., Thomas C., and Derek J. (2005) Segmental Structure of the Brassica Napus Genome Based on Comparative Analysis With Arabidopsis thaliana. Genetics Society of America 171: 765-781.
- Roschzttardtz H., Conejero G., Curie C., Mari S. (2009) Identification of the Endodermal Vacuole as the Iron Storage Compartment in the Arabidopsis Embryo. Plant Physiol. 151: 1329-38.
- Petit, Jean-Michel, Jean-François Briat, and Stéphane Lobréaux. 2001. “Structure and Differential Expression of the Four Members of the *Arabidopsis Thaliana* Ferritin Gene Family.” Biochemical Journal 359 (3): 575. doi:10.1042/0264-6021:3590575.
- Prego, Imelda, Sara Maldonado, and Marisa Otegui. 1998. “Seed Structure and Localization of Reserves in *Chenopodium Quinoa*.” Annals of Botany 82: 481–88. doi:10.1006/anbo.1998.0704.
- Ragland M, Briat JF, Gagnon J, Laulhere JP, Massenet O, Theil EC. 1990. Evidence for conservation of ferritin sequences among plants and animals and for a transit peptide in soybean. The Journal of Biological Chemistry 265: 18339–18344.

- Ravet, Karl, Brigitte Touraine, Jossia Boucherez, Jean François Briat, Frédéric Gaymard, and Françoise Cellier. 2009. “Ferritins Control Interaction between Iron Homeostasis and Oxidative Stress in Arabidopsis.” Plant Journal 57 (3): 400–412. doi:10.1111/j.1365-313X.2008.03698.x.
- Robinson, N J, C M Procter, E L Connolly, and M L Guerinot. 1999. “A Ferric-Chelate Reductase for Iron Uptake from Soils.” Nature 397 (6721): 694–97. doi:Doi 10.1038/17800.
- Roschzttardtz, H., G. Conejero, C. Curie, and S. Mari. 2009. “Identification of the Endodermal Vacuole as the Iron Storage Compartment in the Arabidopsis Embryo.” Plant Physiology 151 (3): 1329–38. doi:10.1104/pp.109.144444.
- Roschzttardtz, H., M. Seguela-Arnaud, J.-F. Briat, G. Vert, and C. Curie. 2011. “The FRD3 Citrate Effluxer Promotes Iron Nutrition between Symplastically Disconnected Tissues throughout Arabidopsis Development.” The Plant Cell 23 (7): 2725–37. doi:10.1105/tpc.111.088088.
- Roschzttardtz, H., and Catherine C. 2009. “Straightforward Histochemical Staining of Fe by the Adaptation of an Old-School Technique.” Plant Signaling & Behavior 5 (1): 56–57. doi:10.1104/pp.109.144444.ron.
- Roschzttardtz, H., Grillet, L., Isaure, M.P., Conéjéro, G., Ortega, R., Curie, C., and Mari, S. 2011. “Plant Cell Nucleolus as a Hot Spot for Iron.” Journal of Biological Chemistry 286 (32): 27863–66. doi:10.1074/jbc.C111.269720.
- Roschzttardtz, H., Bustos, S., Coronas, M. F., Ibeas, M. A., Grant-Grant, S., and Vargas-Pérez, J. (2017) Increasing provasculature complexity in the arabidopsis embryo may increase total iron content in seeds: a hypothesis. Front Plant Sci, 8:960.

- Santi, Simonetta, and Wolfgang Schmidt. 2009. “Dissecting Iron Deficiency-Induced Proton Extrusion in Arabidopsis Roots.” New Phytologist 183 (4): 1072–84. doi:10.1111/j.1469-8137.2009.02908.x.
- Schaaf, Gabriel, Uwe Ludewig, Bülent E. Erenoglu, Satoshi Mori, Takeshi Kitahara, and Nicolaus Von Wirén. 2004. “ZmYS1 Functions as a Proton-Coupled Symporter for Phytosiderophore- and Nicotianamine-Chelated Metals.” Journal of Biological Chemistry 279 (10): 9091–96. doi:10.1074/jbc.M311799200.
- Schnell Ramos, M., Khodja, H., Mary, V., Thomine, S. (2013) Using μPIXE for quantitative mapping of metal concentration in Arabidopsis thaliana seeds. Front Plant Sci, 4:168.
- Soléa V.A., Papillona E., Cottea M., Walterb P., Susini J. (2007) A multiplatform code for the analysis of energy-dispersive X-ray fluorescence spectra. Spectrochimica Acta, 62:63–68.
- Takahashi, Michiko, Tomoko Nozoye, Nobuyuki Kitajima, Naoki Fukuda, Akiko Hokura, Yasuko Terada, Izumi Nakai, et al. 2009. “In Vivo Analysis of Metal Distribution and Expression of Metal Transporters in Rice Seed during Germination Process by Microarray and X-Ray Fluorescence Imaging of Fe, Zn, Mn, and Cu.” Plant and Soil 325 (1): 39–51. doi:10.1007/s11104-009-0045-7.
- Theil, Elizabeth C. 2004. “IRON, FERRITIN, AND NUTRITION.” Annual Review of Nutrition 24 (1): 327–43. doi:10.1146/annurev.nutr.24.012003.132212.
- Vert, G. 2002. “IRT1, an Arabidopsis Transporter Essential for Iron Uptake from the Soil and for Plant Growth.” THE PLANT CELL ONLINE 14 (6): 1223–33. doi:10.1105/tpc.001388.

- Tsai H., Schmidt W. (2017) One way. Or another? Iron uptake in plants. New Phytologist, 214:500-505.
- Walker E., Waters B. (2011) The role of transition metal homeostasis in plant seed development. Curr Opin Plant Biol, 14:318-24.
- Waters, B. M., H.-H. Chu, R. J. DiDonato, L. A. Roberts, R. B. Eisley, B. Lahner, D. E. Salt, and E. L. Walker. 2006. “Mutations in Arabidopsis Yellow Stripe-Like1 and Yellow Stripe-Like3 Reveal Their Roles in Metal Ion Homeostasis and Loading of Metal Ions in Seeds.” Plant Physiology 141 (4): 1446–58. doi:10.1104/pp.106.082586.
- Woolf PJ, Fu LL, Basu A . vProtein: identifying optimal amino acid complements from plant-based foods. *PLoS One* 2011; **6**:e18836.
- Zhu, Wei, Rong Zuo, Rongfang Zhou, Junyan Huang, Minqiang Tang, Xiaohui Cheng, Yueying Liu, et al. 2016. “Vacuolar Iron Transporter BnMEB2 Is Involved in Enhancing Iron Tolerance of Brassica Napus.” Frontiers in Plant Science 7 (September): 1–13. doi:10.3389/fpls.2016.01353.
- Zou, C., Chen, A., Xiao, L. *et al.* A high-quality genome assembly of quinoa provides insights into the molecular basis of salt bladder-based salinity tolerance and the exceptional nutritional value. *Cell Res* **27,** 1327–1340 (2017).